RESEARCH MEMORANDUM

TESTS IN THE AMES 40- BY 80-FOOT WIND TUNNEL OF AN AIRPLANE CONFIGURATION WITH A VARIABLE-INCIDENCE TRIANGULAR WING AND AN ALL-MOVABLE HORIZONTAL TAIL

By David G. Koenig

Ames Aeronautical Laboratory
Moffett Field, Calif.

NATIONAL ADVISORY COMMITTEE FOR AERONAUTICS

WASHINGTON

June 25, 1953

NATIONAL ADVISORY COMMITTEE FOR AERONAUTICS

RESEARCH MEMORANDUM

TESTS IN THE AMES 40- BY 80-FOOT WIND TUNNEL OF AN AIRPLANE CONFIGURATION WITH A VARIABLE-INCIDENCE TRIANGULAR WING AND AN ALL-MOVABLE HORIZONTAL TAIL

By David G. Koenig

SUMMARY

An investigation was made to determine the low-speed, large-scale characteristics of an airplane configuration with an aspect ratio 2 triangular wing of variable incidence. The complete model consisted of the variable-incidence wing in combination with a fuselage of fineness ratio 13 (in plan view), a triangular vertical tail, and a thin, unswept, all-movable horizontal tail. The wing had an NACA 0005 (modified) section and was equipped with partial-span, slotted, trailing-edge flaps. Tests of the model at zero sideslip for 0°, 6°, 10°, and 14° wing incidences were made with the horizontal tail off and with the horizontal tail at each of three vertical positions above the fuselage reference plane. Characteristics of the model in sideslip were obtained for a wing incidence of 10° with two combinations of flap and horizontal-tail settings. The average Reynolds number based on the mean aerodynamic chord was 14.7 million and the Mach number was 0.13.

The results of tests of the model with the horizontal tail off showed that wing incidence was approximately 87 percent as effective in producing lift on the model as was angle of attack. The effect of wing incidence on flap lift effectiveness was about the same as that due to model angle of attack.

Results of tests of the model with the tail installed showed that, in general, increasing wing incidences were accompanied by increases in the extent of instability throughout the lift-coefficient range. This is related to the adverse effects on stability of increases in tail height above the wing-chord plane due to wing incidence.

Use of the wing as a trimming device with the tail fixed produced stability but showed no advantage in lift over that possible for the model with the flaps deflected and with the wing undeflected. Slight increases in drag accompanied use of the wing as a trimming device.

With the wing deflected 10°, directional instability was found to occur at approximately the same lift coefficient as was the case for a similar model with the wing at zero incidence.

INTRODUCTION

Problems have arisen from the undesirably high attitudes used to attain landing lift coefficients for low-aspect-ratio triangular-wing airplane configurations. Two methods which have been investigated for reducing the attitudes required are the use of trailing-edge flaps and the use of a variable-incidence wing. High-lift, trailing-edge flaps have been investigated at high Reynolds numbers on an airplane model having a triangular wing of aspect ratio 2 and an all-movable horizontal tail (refs. 1 and 2). Wing-fuselage models with variable-incidence wings of aspect ratio 2 have been tested at low Reynolds number (ref. 3).

In order to extend the scope of published data on triangular-wing models with variable-incidence wings to higher Reynolds number, and for the purpose of investigating the static stability of a variable-incidence triangular-wing model equipped with a horizontal and vertical tail, tests were made in the 40- by 80-foot wind tunnel on a model with an aspect ratio 2 triangular wing, a horizontal tail and vertical tail identical to the model reported in references 1 and 2, but with the fuselage modified to accommodate the varying of the wing incidence.

NOTATION

Figure 1 shows the sign convention used for presentation of the data. All control-surface deflections are measured in a plane perpendicular to the hinge or pivot line of the control surface.

b	wing span, ft
b_f	flap span (movable), ft
b_t	horizontal-tail span, ft
c	wing chord, measured parallel to wing center line, ft
$\bar{c}$	mean aerodynamic chord of wing, measured parallel to wing center line, $\frac{\int_0^{b/2} c^2 dy}{\int_0^{b/2} c\, dy}$, ft

[redacted]

C_D	drag coefficient, $\frac{\text{drag}}{qS}$
C_{D_T}	increment of drag coefficient due to wind-tunnel-wall interference
C_l	rolling-moment coefficient, $\frac{\text{rolling moment}}{qSb}$
C_L	lift coefficient, $\frac{\text{lift}}{qS}$
C_m	pitching-moment coefficient, $\frac{\text{pitching moment}}{qS\bar{c}}$
C_{m_t}	horizontal-tail contribution to the pitching-moment coefficient of the model at a given angle of attack
C_{m_T}	increment of horizontal-tail contribution to the pitching moment due to wind-tunnel-wall interference
C_n	yawing-moment coefficient, $\frac{\text{yawing moment}}{qSb}$
C_Y	side-force coefficient, $\frac{\text{side force}}{qS}$
D	total drag, lb
i_t	horizontal-tail incidence relative to the fuselage reference plane, deg
i_w	wing incidence relative to the fuselage reference plane (positive direction same as for α), deg
l_t	distance from moment center to pivot line of the horizontal tail, ft
L	total lift, lb
$\frac{L}{D}$	lift-drag ratio
S	total wing area, sq ft
S_f	trailing-edge-flap area (total movable), sq ft
S_t	horizontal-tail area, sq ft
W	fuselage width, ft

[redacted]

x	longitudinal coordinate parallel to the model plane of symmetry and the fuselage reference plane, ft
y	lateral coordinate perpendicular to the model plane of symmetry, ft
z	vertical coordinate perpendicular to the fuselage reference plane, ft
z_t	vertical coordinate perpendicular to the wing-chord plane, ft
α	angle of attack of the fuselage reference plane with reference to free stream, deg
α_T	increment of angle of attack due to wind-tunnel-wall interference, deg
β	angle of sideslip of the model plane of symmetry with reference to free stream, deg
δ_f	flap deflection with reference to the wing-chord plane, deg
Δ	symbol denoting increment
$C_{L_{i_w}}$	$\left(\frac{\partial C_L}{\partial i_w}\right)_{\alpha=0}$
C_{L_α}	$\left(\frac{\partial C_L}{\partial \alpha}\right)_{i_w=0}$

MODEL

A drawing of the model is shown in figure 2 and pertinent geometric data are presented in table I. A photograph of the model as mounted in the Ames 40- by 80-foot wind tunnel is presented in figure 3.

The wing sections parallel to the model center line were modified NACA 0005 sections. The modification consisted of a straight fairing from the 67-percent-chord station back to the trailing edge. The ordinates of the modified NACA 0005 section are presented in table II. The wing-fuselage installation was such as to allow changing the wing incidence through a range of 0° to 14°. The wing was pivoted about a line located at the 0.25-chord point of the mean aerodynamic chord and lying in the fuselage reference plane and was equipped with partial-span, constant-percent-chord, slotted flaps. Dimensions of the flaps are presented in figure 4.

[redacted]

Geometric data on the fuselage are presented in figure 5. In the fuselage reference plane, the fineness ratio is 13.00. The depth of the fuselage was such as to maintain a wing-fuselage gap (at the juncture of the wing and fuselage) of 0.0008 b/2 or less for wing incidences of 0° to 10°. At 14° wing incidence, the wing-fuselage gap was 0.0008 b/2 or less from the wing leading edge back to approximately the 70-percent-chord station, from which the gap increased to a value of 0.0047 b/2 at the trailing edge of the wing.

The horizontal and vertical tails were identical to those of the model reported in references 1 and 2. Characteristics of the model were obtained with the horizontal tail at each of three vertical positions, hereinafter to be referred to as low, middle, and high position, with values of $z/(b/2)$ of 0, 0.25, and 0.50, respectively.

In the low position, the horizontal tail had a larger span ($b_t/b = 0.738$) than in the middle and high positions ($b_t/b = 0.632$).

All wing and horizontal-tail deflections were within ±0.1°. Flap settings were made within ±0.2°.

TESTS

Longitudinal characteristics of the model with the horizontal tail off were obtained with the wing at several angles of incidence and the flaps undeflected and deflected 40°. Longitudinal characteristics of the model with the horizontal tail installed (i_t, 0°) at each of the three positions (for values of $z/(b/2)$ of 0, 0.25, and 0.50) were obtained for several wing incidences with the flaps undeflected. With the tail in the low position and for δ_f, 0°, tests were made with the tail set at incidences other than 0°. With the flaps deflected 40° and with the tail in the low position, tests were made for several wing incidences at i_t, 0° and for tail incidences other than 0° at i_w, 0° and 10°.

A limited investigation of the sideslip characteristics of the model was made with the horizontal tail in the low position and with the wing at 10° incidence. Flap and tail setting combinations used were δ_f, 0°, i_t, 0°, and δ_f, 40°, i_t, 10° which were chosen to provide longitudinal trim at a landing lift coefficient. Tests were made with varying angle of attack at several angles of sideslip, and with varying angle of sideslip for several angles of attack.

The average Reynolds number of the tests was 14.7 million based on the mean aerodynamic chord. The dynamic pressure was approximately 25 pounds per square foot and the Mach number was 0.13.

[redacted]

CORRECTIONS TO DATA

All the data were corrected for air-stream inclination and for wind-tunnel-wall effects, the latter correction being that for a wing of the same span having elliptic loading but with an unswept plan form. These corrections were made as follows:

$$\alpha_T = 0.73\ C_L$$

$$C_{D_T} = 0.0128\ C_L^2$$

For data with the horizontal tail installed, a correction for additional downwash at the pivot line of the tail (at the plane of symmetry, β, 0°) was made as follows:

$C_{m_T} = 0.0100\ C_L$ for the model with the tail in the low position

$C_{m_T} = 0.0093\ C_L$ for the model with the tail in the middle and high positions

Drag and pitching-moment tares due to strut interference, based on data obtained with a rectangular wing, were applied to the data.

RESULTS AND DISCUSSION

The basic results of the investigation are presented in figures 6 through 14, and table III may be used as an index to these figures. The data were corrected for wind-tunnel-wall effects and support-strut interference.

For purposes of aiding in the comparison of the longitudinal characteristics of the model with the horizontal tail at each of the tail positions, moment center locations were chosen such that a value of $(dC_m/dC_L)_{C_L=0}$, -0.06 would be obtained with the wing at 0° incidence and the flaps and horizontal tail undeflected. These moment centers were located at 41.8, 46.2, and 53.0 percent of the mean aerodynamic chord for the low, middle, and high positions, respectively. For the pitching-moment data with the horizontal tail off, a moment center location of 25-percent mean aerodynamic chord was used.

Lift Characteristic of the Model With Tail Off

The effectiveness of wing incidence in producing lift of the model as compared to that produced by model angle of attack is presented in figure 15. Wing incidence was less effective in producing lift than was angle of attack; $C_{L_{i_w}}/C_{L_\alpha}$ was approximately 0.87 for both 0° and 40° flap deflections.

The effects of wing incidence on flap lift effectiveness are shown in figure 16. Qualitatively, the main effect of wing incidence is shown to be equivalent to that of actual wing angle of attack $(\alpha + i_w)$; the flap lift increment decreased rapidly when $\alpha + i_w$ exceeded approximately 16°.

Longitudinal Stability With the Horizontal Tail On

Figure 17 shows the effect of wing incidence on the longitudinal stability of the model with the horizontal tail at each of three tail heights with respect to the fuselage reference plane. A comparison of the pitching-moment curves of figure 17 indicates that the changes in stability brought about by wing-incidence changes with the horizontal-tail height fixed are, in general, similar to the changes resulting from an increase in tail height with the wing incidence fixed.

The loss in stability when the wing incidence is increased from 0° to 10° is attributable directly to the height of the horizontal tail above the wing-chord plane. This is indicated by the data of figure 18 which presents the pitching-moment contribution of the horizontal tail, C_{m_t}, as a function of $\alpha + i_w$, for the tail at a given tail height above the wing-chord plane with the wing at 0° and 8° incidence. Although a difference in tail span and tail incidence with respect to the wing contribute to a quantitative disagreement of the two curves, the shapes of the two curves are approximately the same. Figure 18 thus demonstrates that the effect of wing incidence on the stability characteristics of the model is the result of the accompanying change in tail height above the chord plane.

Examination of the data of figure 7 indicates the possibility of avoiding the adverse effect of wing incidence on the longitudinal stability of the model with the tail in the low position. This could be done by varying the wing incidence to provide longitudinal trim. It is seen from figure 7 that the model would be stable at the trim condition.

[redacted]

Trim Lift and Drag Characteristics

Trim characteristics are presented in figure 19 for the model with the wing used as a trimming device with the tail fixed (i_t, 0°) and for the model with the tail used to maintain trim but with the wing undeflected. The figure shows that with the flaps deflected, an insignificant amount of trim lift is gained by using wing incidence. With the flaps retracted, the trim lift coefficients at angles of attack below that for maximum lift of the model with variable-incidence wing were less than those obtained with the wing fixed and the flaps deflected.

The model with variable-incidence wing showed approximately the same trim drag characteristics as did the fixed-wing model for values of C_L below 0.9 and 1.1 for δ_f, 0° and 40°, respectively. For lift coefficients above these values, the variable-incidence model had slightly higher drag than that of the fixed-wing model.

Directional Instability

The data for the model of reference 2 (similar to the present model except for fuselage shape) showed that directional instability occurred at lift coefficients of the order of 1.2. It is believed that this directional instability was due to sidewash induced by separation vortices originating from the wing (see ref. 4). Based on the reasoning expressed in reference 4, it would be expected that with an increase in wing incidence, the vertical tail would be in a region of less adverse sidewash. Results of the present investigation show, however, that with the wing at 10° incidence, directional instability still occurs at approximately the same lift coefficient as for the model (i_w, 0°) of reference 2.

CONCLUDING REMARKS

Results of the investigation of the model with the horizontal tail off showed that wing incidence was approximately 87 percent as effective in producing lift as was model angle of attack. The effect of wing incidence on flap lift effectiveness was approximately the same as that due to model angle of attack.

Results of the tests of the model with the tail installed showed that setting the wing at incidence had an adverse effect on longitudinal stability. The adverse effect was the result of increases in tail height above the wing-chord plane produced by increases in wing incidence. The tail-height change due to wing incidence was shown to have approximately the same effect as changing the tail height with the wing incidence held constant.

[redacted]

Trimming the model by varying the wing incidence rather than using the tail as a trimming device produced no significant advantages in lift over that possible for the model with the wing undeflected but equipped with high lift flaps. Trimmed by varying the wing incidence, the model was longitudinally stable for the entire trim lift range for the moment center locations and tail incidences considered. The trim drag characteristics were not affected greatly by using the wing as a trim device.

With the wing deflected 10°, directional instability was found to occur at approximately the same lift coefficient as was the case for a similar model with the wing at zero incidence.

Ames Aeronautical Laboratory
National Advisory Committee for Aeronautics
Moffett Field, Calif.

REFERENCES

1. Graham, David, and Koenig, David G.: Tests in the Ames 40- by 80-Foot Wind Tunnel of an Airplane Configuration With an Aspect Ratio 2 Triangular Wing and an All-Movable Horizontal Tail - Longitudinal Characteristics. NACA RM A51B21, 1951.

2. Graham, David, and Koenig, David G.: Tests in the Ames 40- by 80-Foot Wind Tunnel of an Airplane Configuration With an Aspect Ratio 2 Triangular Wing and an All-Movable Horizontal Tail - Lateral Characteristics. NACA RM A51L03, 1952.

3. Hopkins, Edward J., and Carel, Hubert C.: Experimental and Theoretical Study of the Interference at Low Speed Between Slender Bodies and Triangular Wings. NACA RM A53A14, 1953.

4. Anderson, Adrien E.: An Investigation at Low Speed of a Large-Scale Triangular Wing of Aspect Ratio Two.- III. Characteristics of Wing with Body and Vertical Tail. NACA RM A9H04, 1949.

[redacted]

TABLE I.- GEOMETRIC DATA OF MODEL

Wing	
Area, total, sq ft	312.5
Area, movable (exposed), sq ft	215.96
Span, ft	25.00
Mean aerodynamic chord, ft	16.67
Aspect ratio	2
Taper ratio	0
Airfoil section parallel to model center line	NACA 0005 (modified)
Fuselage	
Length, ft	56.16
Maximum width (on wing-chord plane), ft	4.32
Fineness ratio (in chord plane)	13.00
Vertical tail	
Exposed area, sq ft	52.53
Aspect ratio	1
Taper ratio	0
Airfoil section parallel to model center line	NACA 0005 (modified)
Trailing-edge flaps	
S_f/S	0.123
Chord	0.2084c
Horizontal tail	
Low position	
S_t/S	0.246
b_t/b	0.738
$l_t/\bar{c}$ (c.g. at 0.418$\bar{c}$)	1.170
$z/(b/2)$ (i_w, 0°)	0
Aspect ratio	4.4
Taper ratio	0.46
Middle position	
S_t/S	0.200
b_t/b	0.632
$l_t/\bar{c}$ (c.g. at 0.462$\bar{c}$)	1.125
$z/(b/2)$ (i_w, 0°)	0.25
Aspect ratio	4.0
Taper ratio	0.50
High position	
S_t/S	0.200
b_t/b	0.632
$l_t/\bar{c}$ (c.g. at 0.530$\bar{c}$)	1.057
$z/(b/2)$ (i_w, 0°)	0.50
Aspect ratio	4.0
Taper ratio	0.50

[redacted]

NACA

TABLE II.- COORDINATES OF THE NACA 0005 (MODIFIED) SECTION

Station (percent chord)	Ordinate (percent chord)
0	0
1.25	.789
2.50	1.089
5.00	1.481
7.50	1.750
10.00	1.951
15.00	2.228
20.00	2.391
25.00	2.476
30.00	2.501
40.00	2.419
50.00	2.206
60.00	1.902
67.00	1.650
70.00	1.500
80.00	1.000
90.00	.500
100.00	0
L.E. radius: 0.275-percent chord	

TABLE III.- INDEX OF CONFIGURATIONS TESTED

[W, wing; F, fuselage; V, vertical tail; HL, HM, HH, horizontal tail at low, middle, high position, respectively]

Figure	Configuration	Control deflection, deg			β deg	α deg	Data
		i_w	δ_f	i_t			
6(a),(b)	W+F+V	0,6,10,14	0,40	tail off	0	-2 to 26	C_L vs α, C_D, C_m
7(a),(b)	W+F+V+HL	0,6,10,14	0,40	0	0	-2 to 26	C_L vs α, C_D, C_m
8	W+F+V+HM	0,6,10,14	0	0	0	-2 to 26	C_L vs α, C_D, C_m
9	W+F+V+HH	0,6,10,14	0	0	0	-2 to 25	C_L vs α, C_D, C_m
10(a),(b),(c),(d)	W+F+V+HL	0,10	0,40	-2 to 10	0	-2 to 26	C_L vs α, C_D, C_m
11(a),(b)	W+F+V+HL	10	0	0	0,6,8	0 to 26	C_L vs α, C_D, C_m C_l, C_n, C_Y
12(a),(b)	W+F+V+HL	10	0	0	-4 to 8	0,9,17 21	C_L, C_D, C_m, C_Y, C_n, C_l, vs β
13(a),(b)	W+F+V+HL	10	40	10	0,6,8	0 to 25	C_L vs α, C_D, C_m C_l, C_n, C_Y
14(a),(b)	W+F+V+HL	10	40	10	-4 to 8	1,9,17 21	C_L, C_D, C_m, C_Y, C_n, C_l, vs β

[redacted]

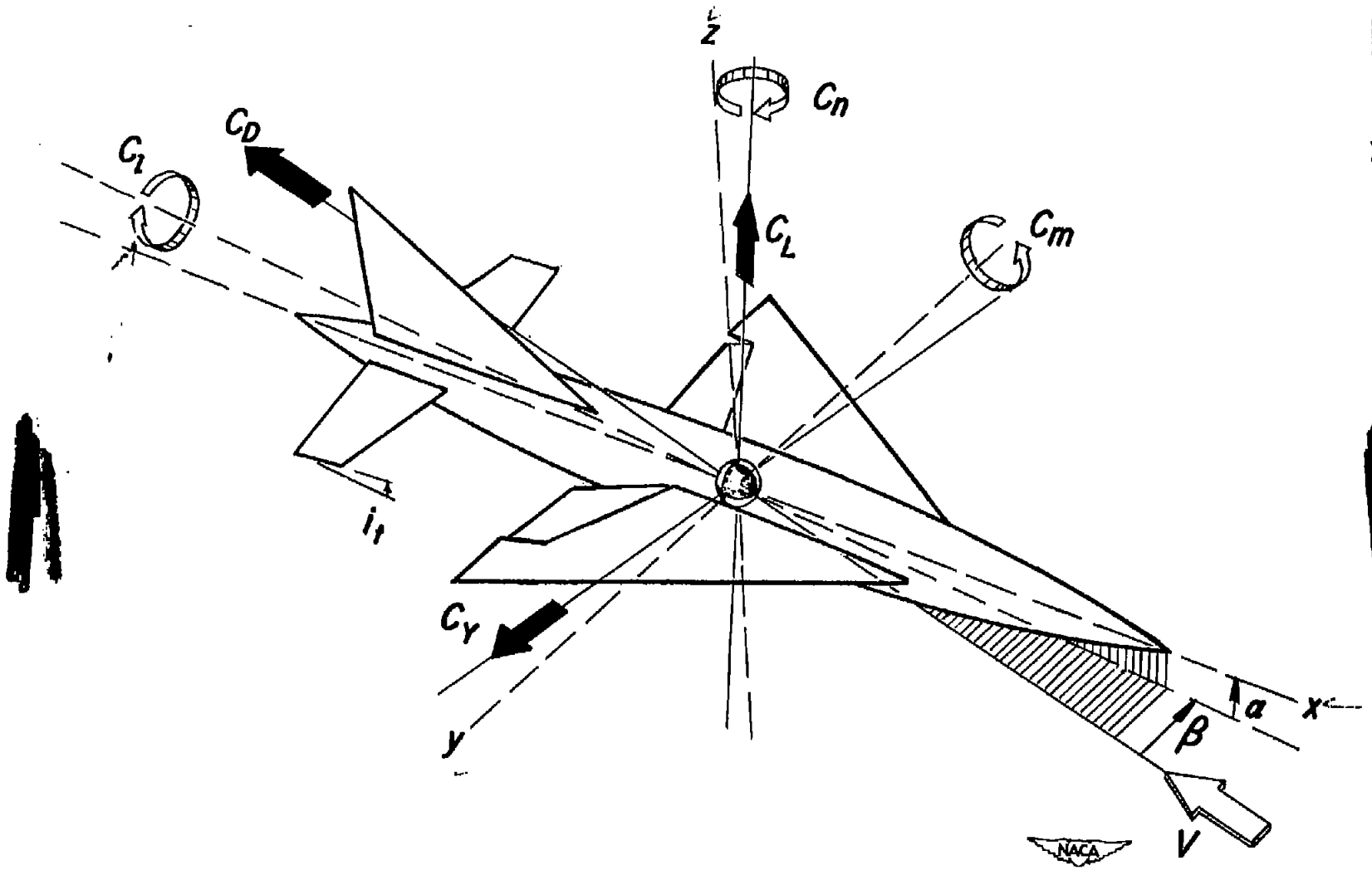

Figure 1.- The sign convention used in presentation of the data. All force and moment coefficients, angles, and control-surface deflections are shown as positive.

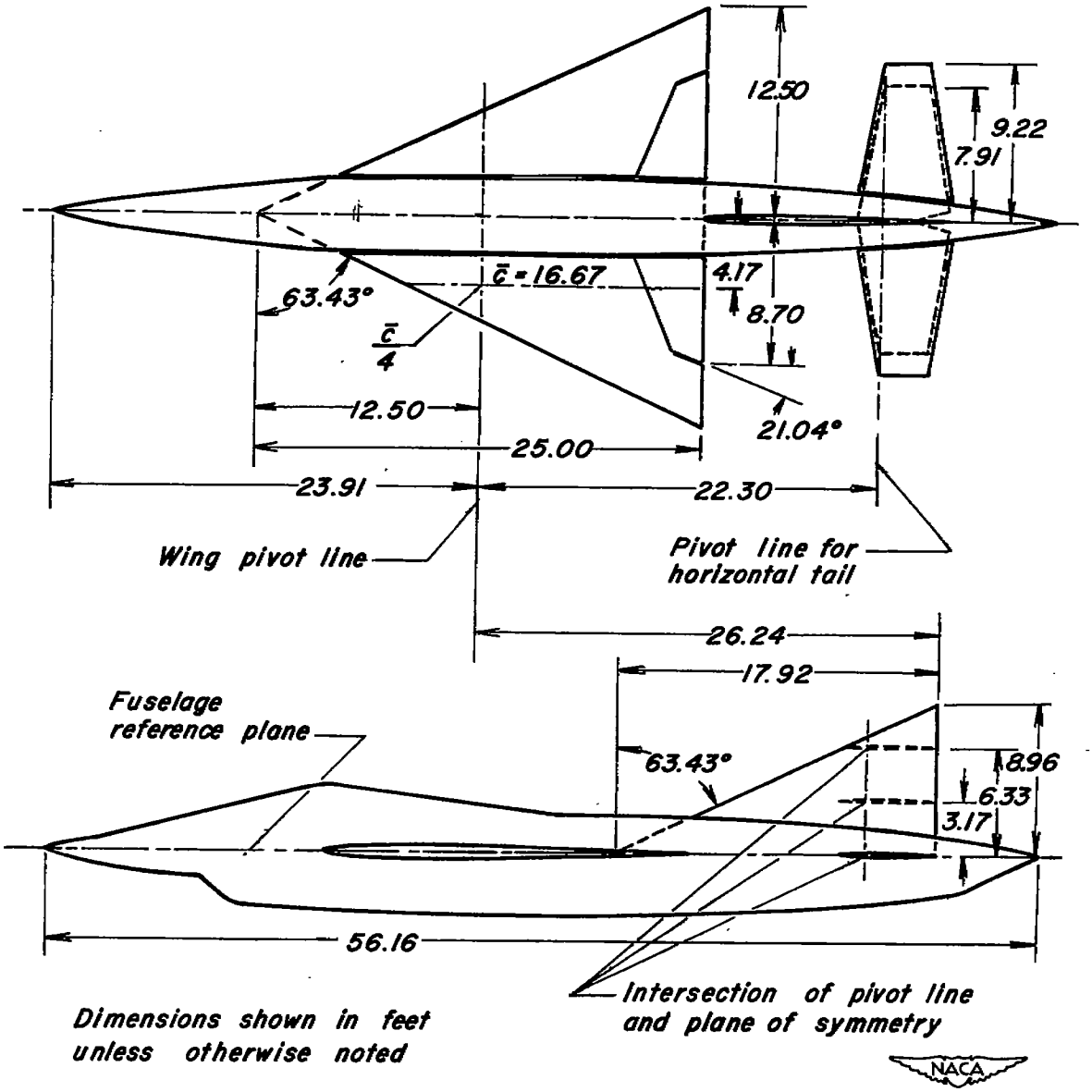

Figure 2.- Geometric details of the model, wing at 0° incidence.

[redacted]

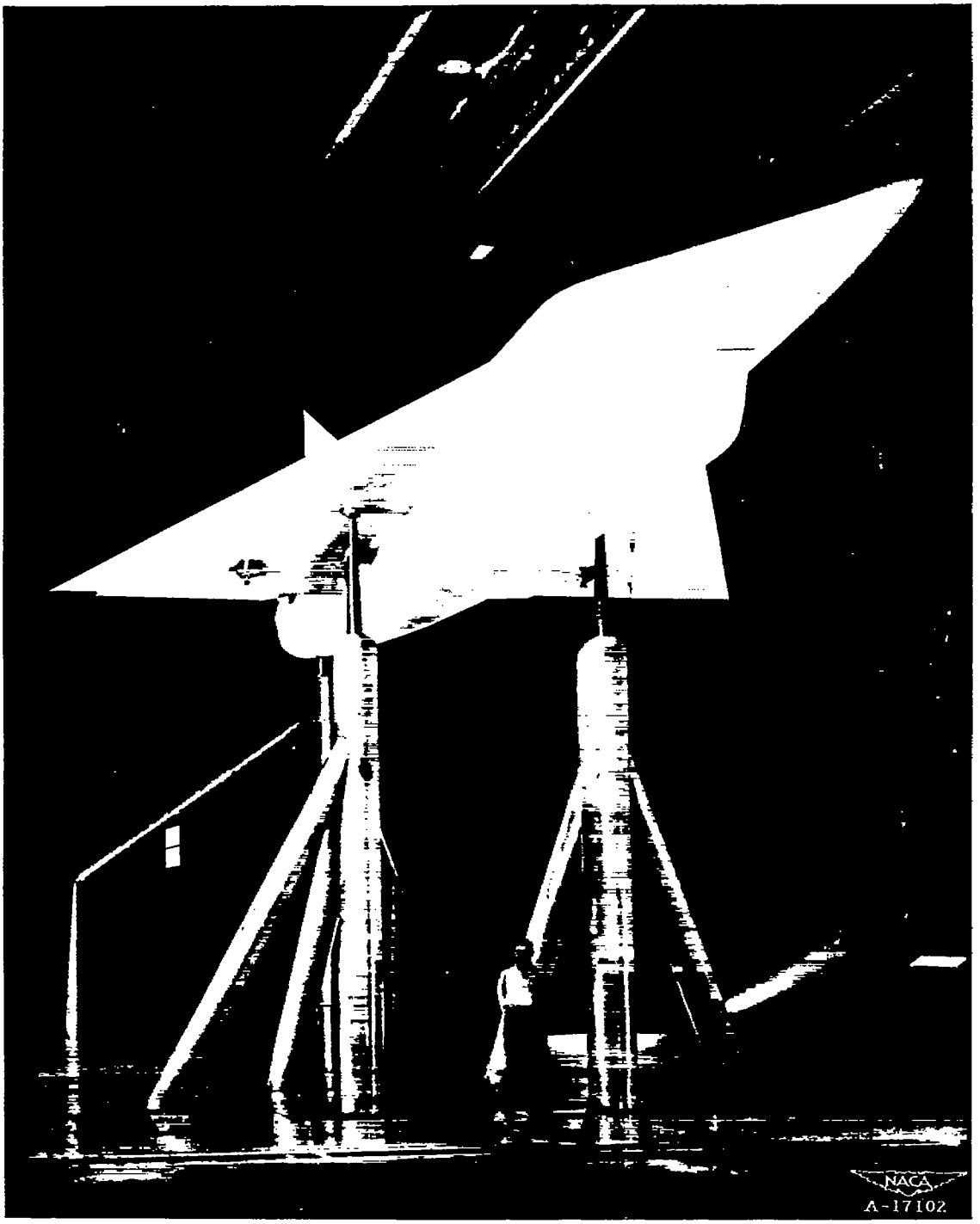

Figure 3.- The model as mounted in the Ames 40- by 80-foot wind tunnel, shown with the wing at 10° incidence.

[redacted]

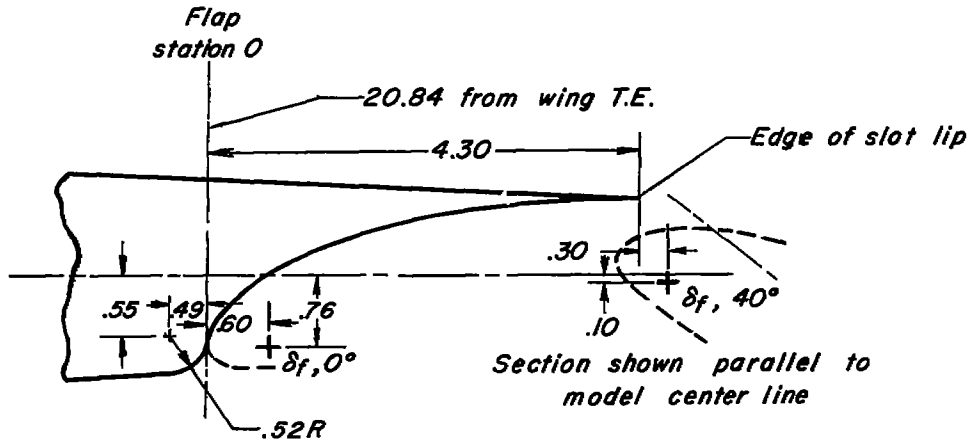

+ Point at which flap hinge line intersects section plane. Flap deflection, δ_f, is measured perpendicular to flap hinge line.

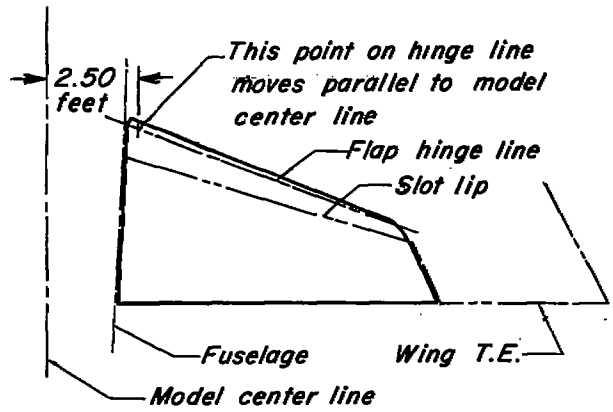

Flap coordinates		
Station	Upper surface	Lower surface
0	-0.77	-0.77
.10	- .49	- .91
.20	- .36	- .96
.40	- .16	- .99
.60	- .01	-1.00
1.20	.31	- .99
1.80	.52	- .96
2.40	.66	- .92
3.00	.76	- .89
3.60	.80	- .86
4.20	.81	- .83
5.00	.80	- .80
10.00	.54	- .54
15.00	.29	- .29
20.84	0	0
Center of L.E. arc		
.15	- .77	
L.E. radius: 0.15		

NACA

Dimensions shown in percent wing chord

Figure 4.- Geometric data of the trailing-edge constant-percent-chord slotted flap.

[redacted]

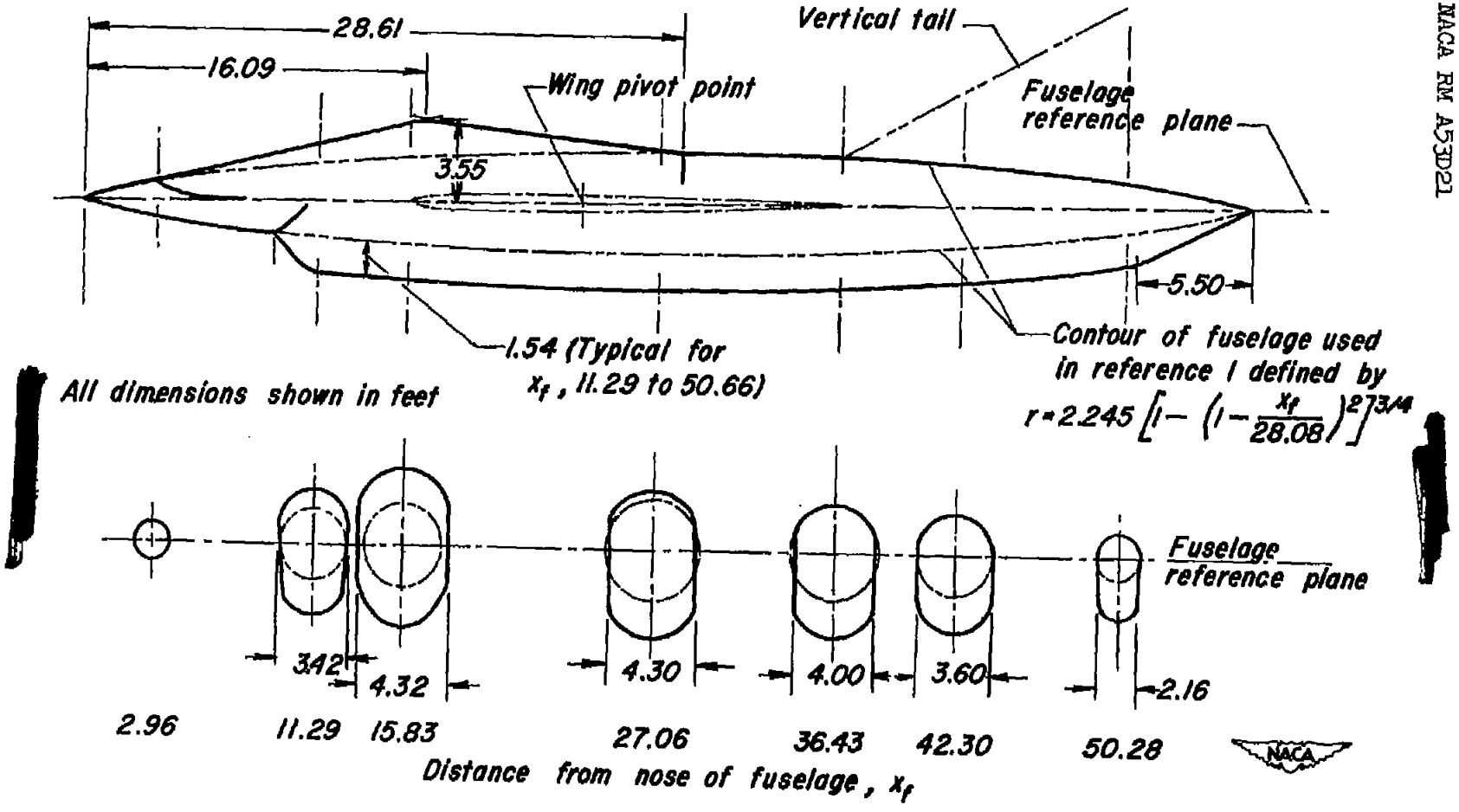

Figure 5.- Geometric details of the fuselage.

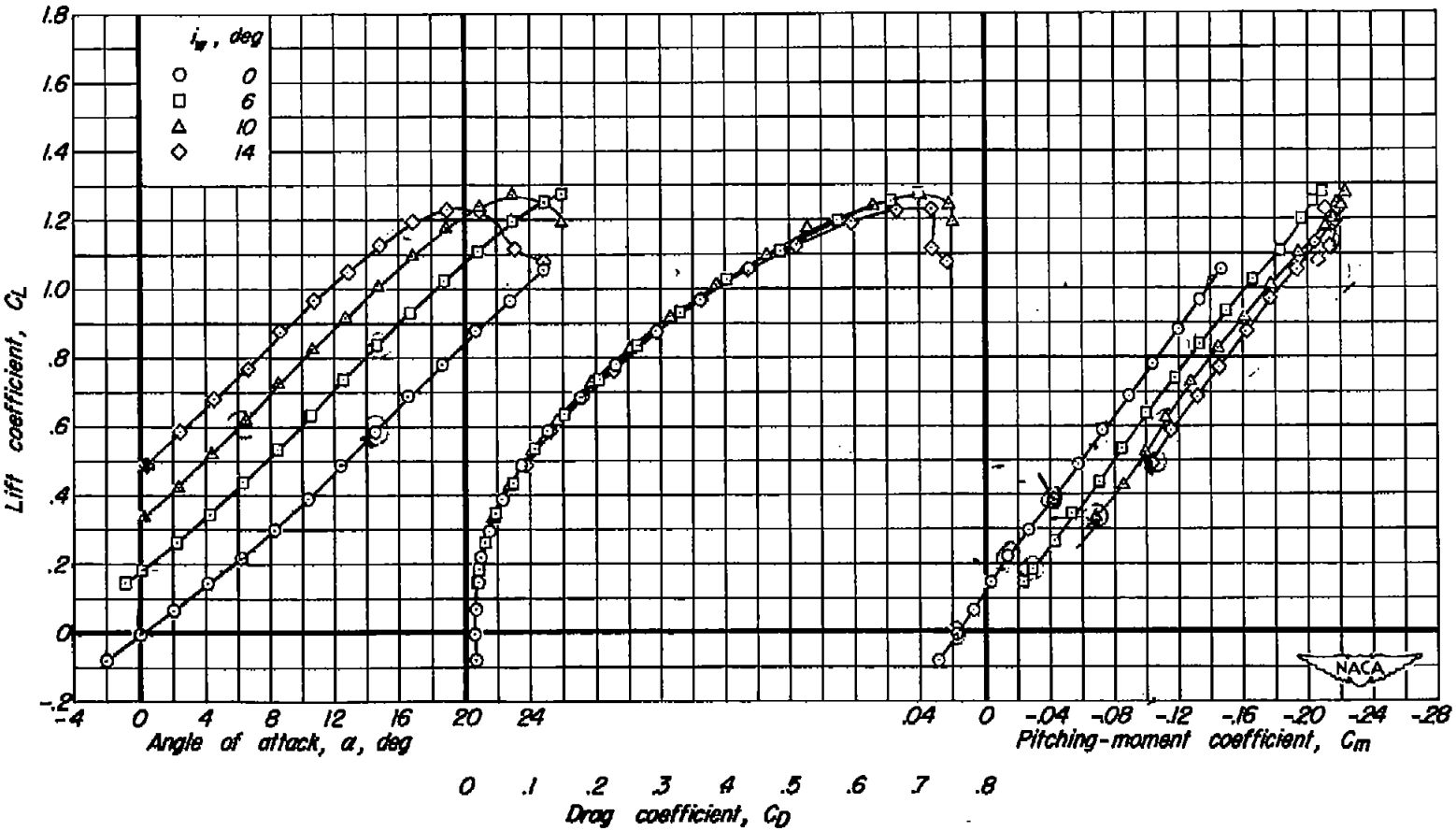

(a) δ_f, 0°

Figure 6.- Longitudinal characteristics of the model with the wing at four incidences and the tail off; moment center, 0.250$\bar{c}$.

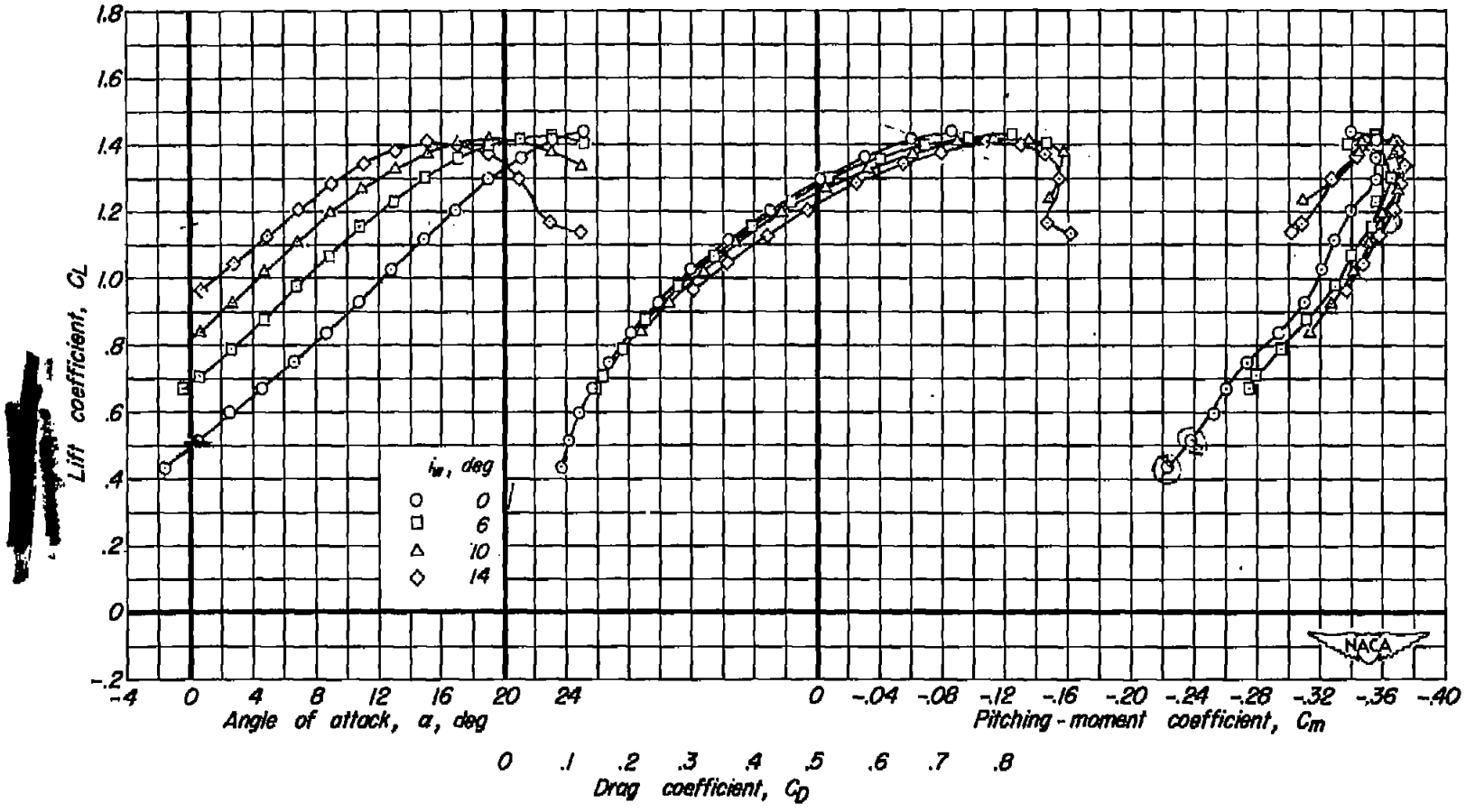

(b) δ_f, 40°

Figure 6.- Concluded.

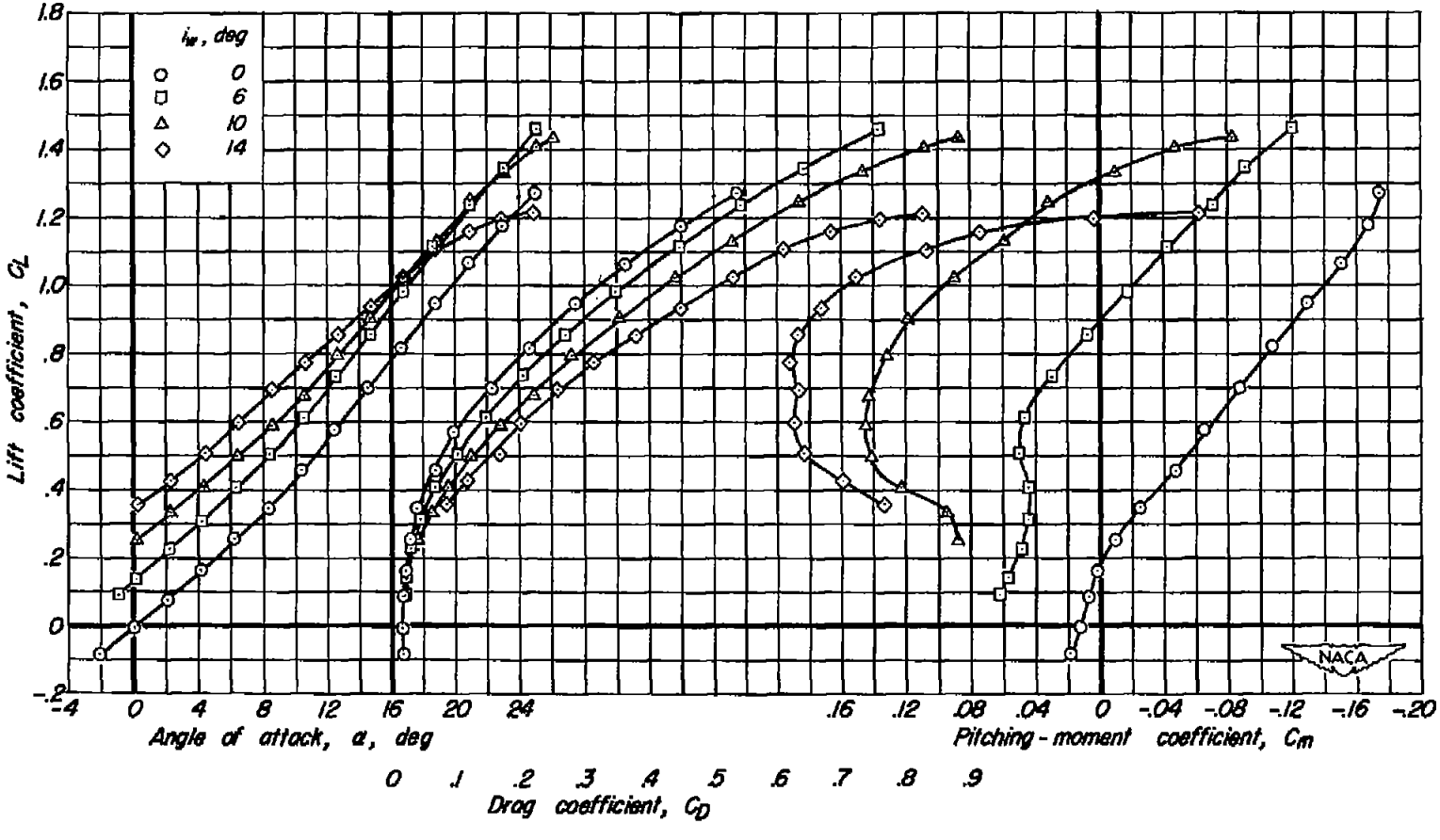

(a) δ_f, 0°

Figure 7.- Longitudinal characteristics of the model with the wing at four incidences and the tail in the low position; i_t, 0°; z/(b/2), 0; moment center, 0.418$\bar{c}$.

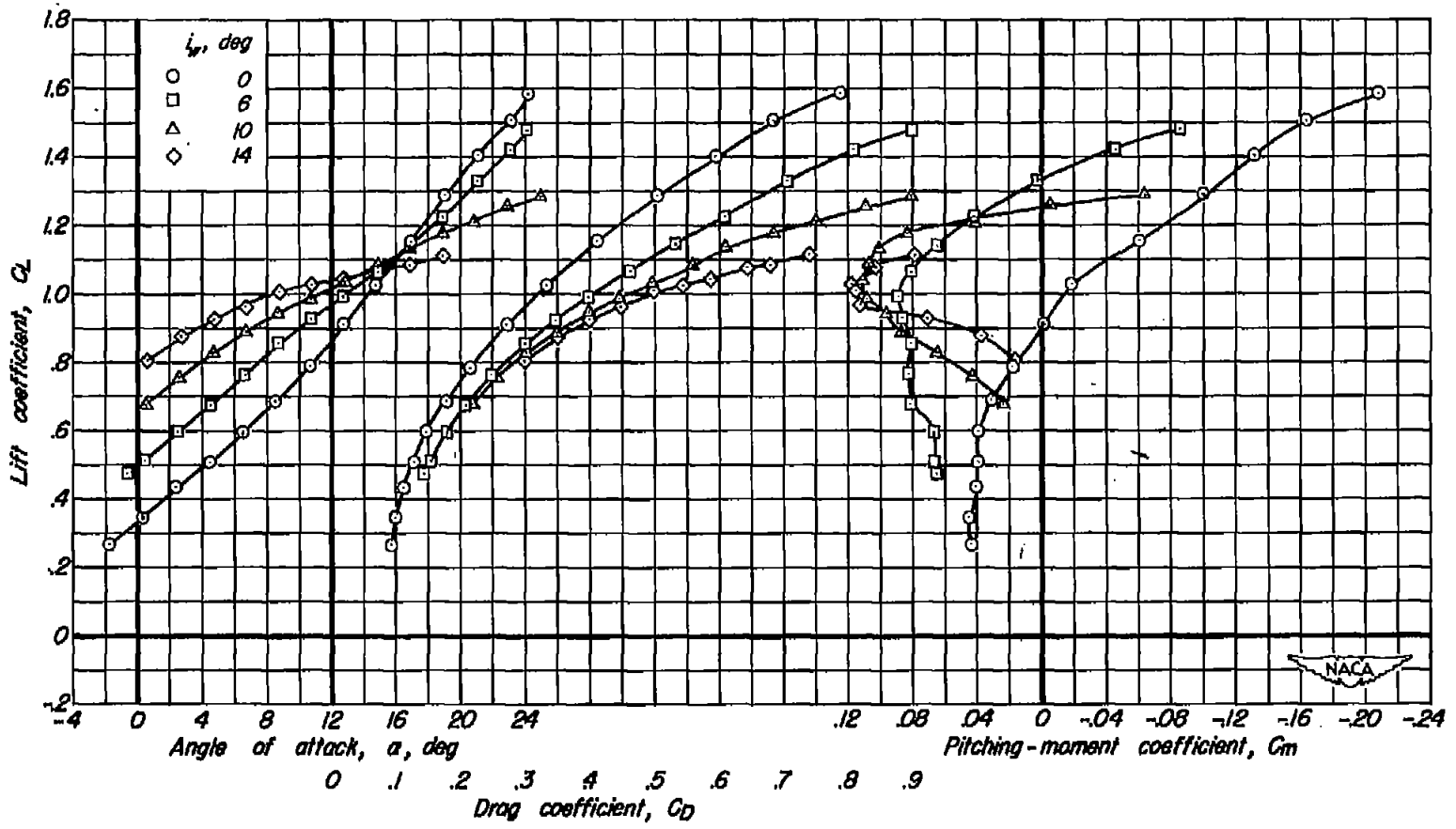

(b) δ_f, 40°

Figure 7.- Concluded.

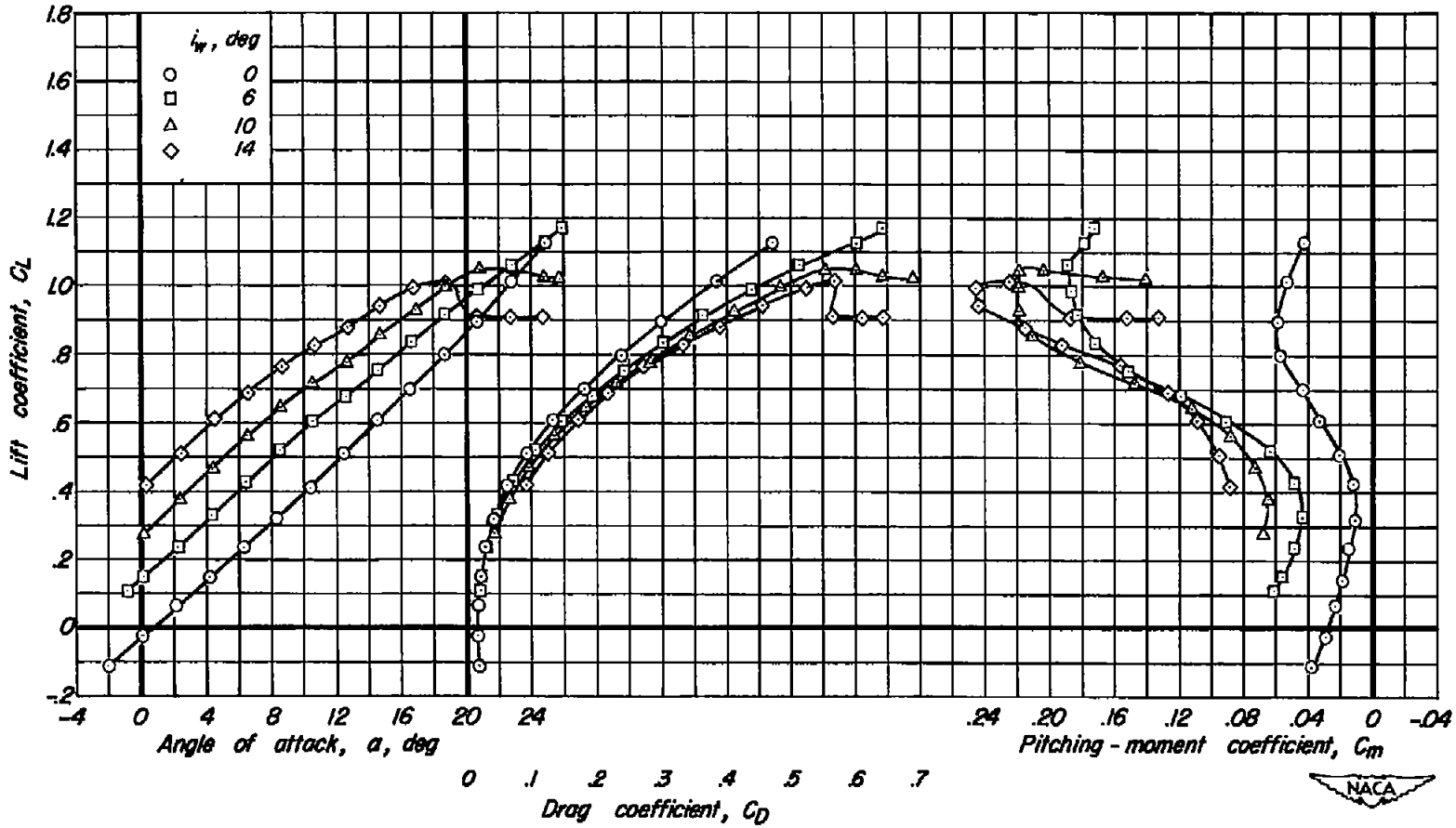

Figure 8.- Longitudinal characteristics of the model with the wing at four incidences, the flaps retracted, and the horizontal tail in the middle position; i_t, 0°; z/(b/2), 0.25; moment center, 0.462$\bar{c}$.

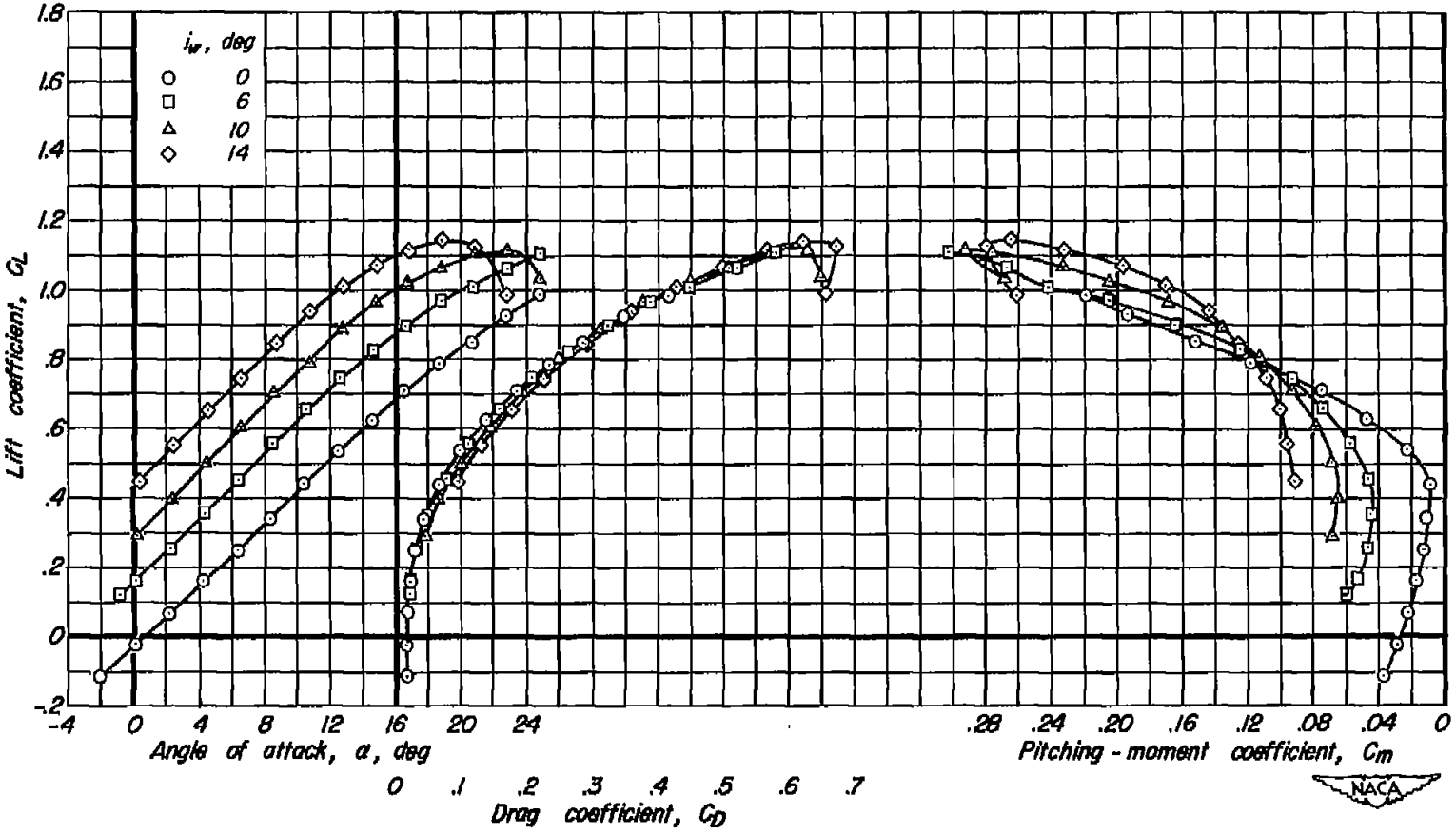

Figure 9.- Longitudinal characteristics of the model with the wing at four incidences, the flaps retracted, and the horizontal tail in the high position; i_t, 0°; z/(b/2), 0.50; moment center, 0.530$\bar{c}$.

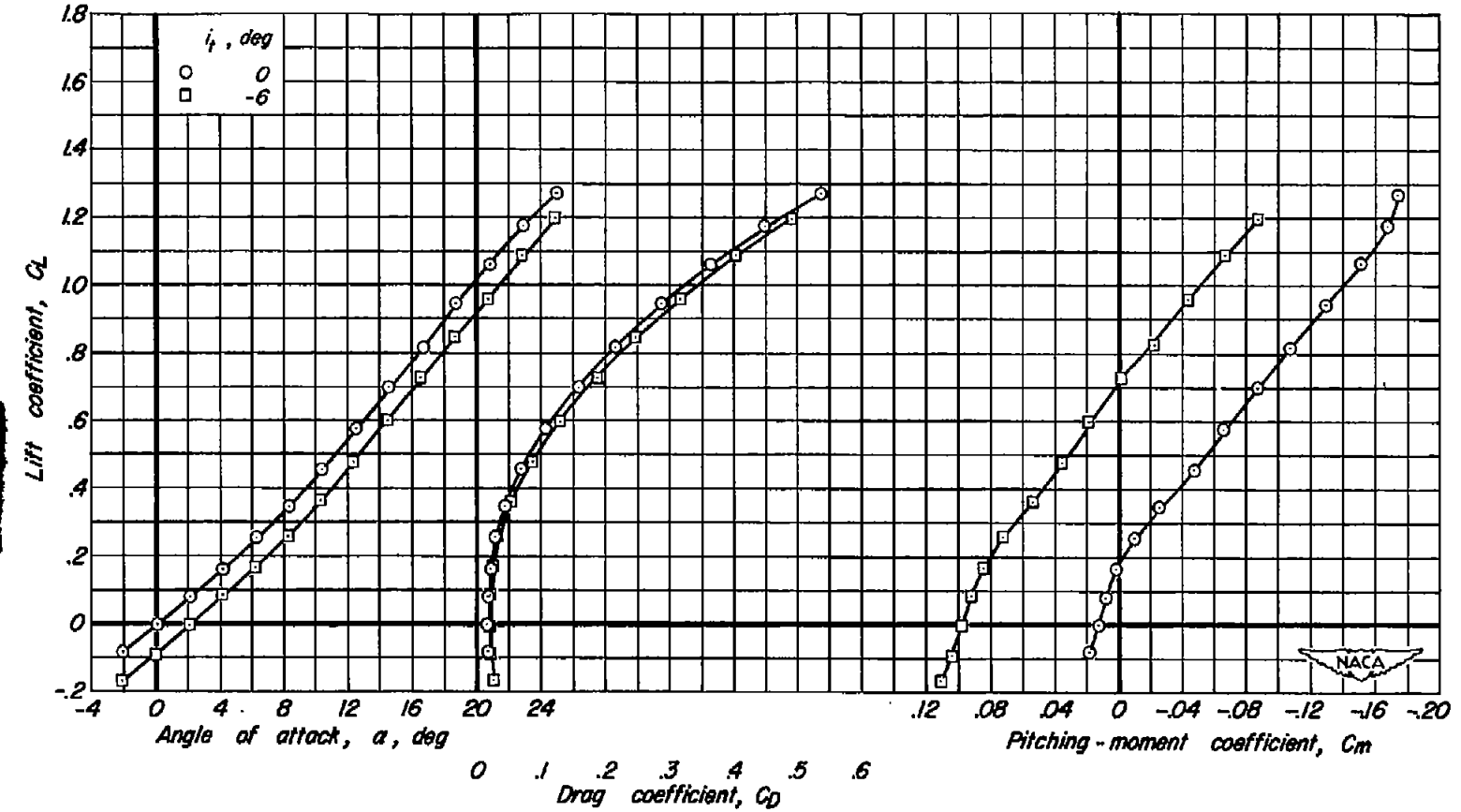

(a) i_w, 0°; δ_f, 0°

Figure 10.- The effect of tail incidence on the longitudinal characteristics of the model with the tail in the low position; z/(b/2), 0; moment center, 0.418$\bar{c}$.

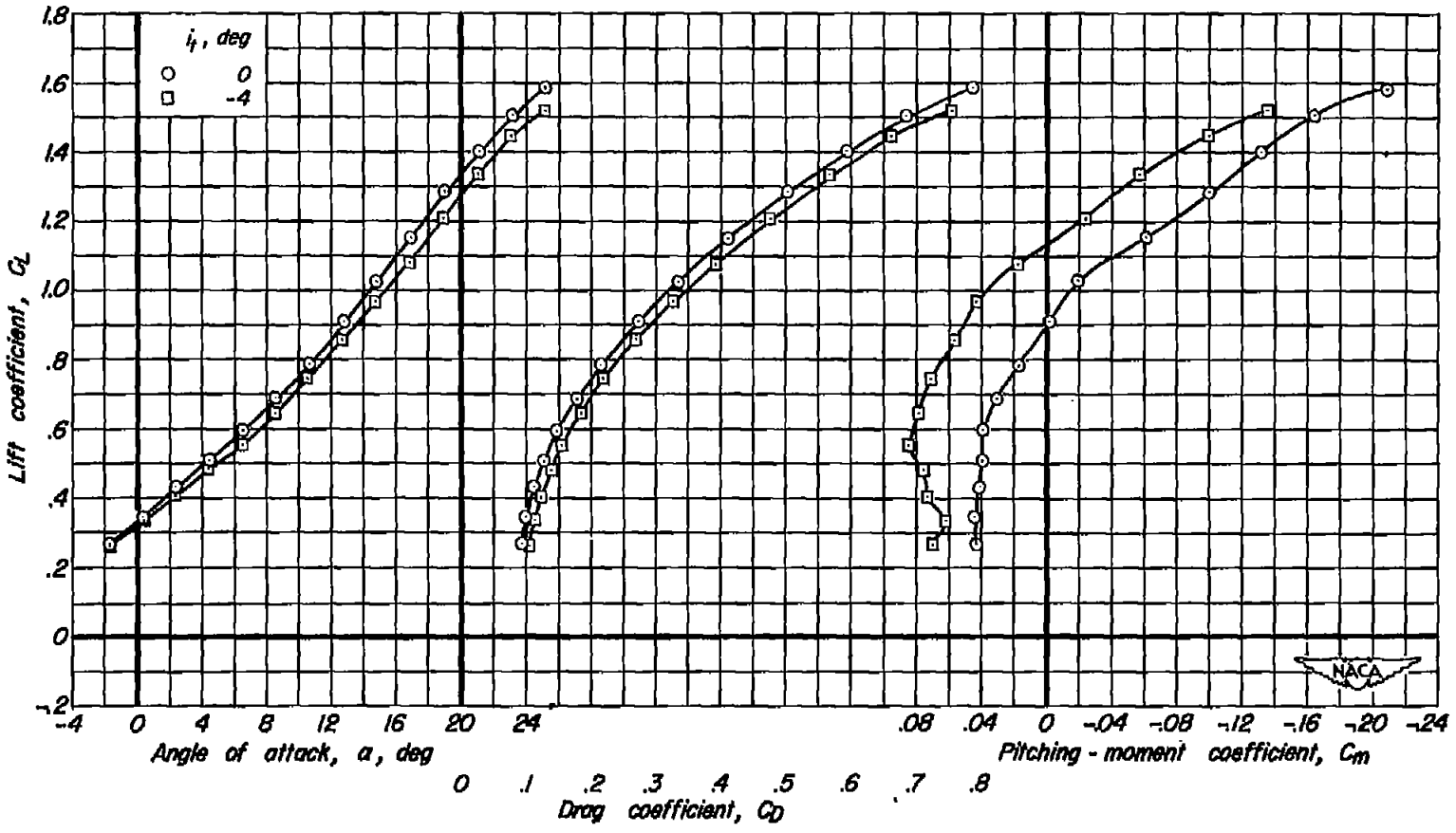

(b) i_w, 0°; δ_F, 40°

Figure 10.- Continued.

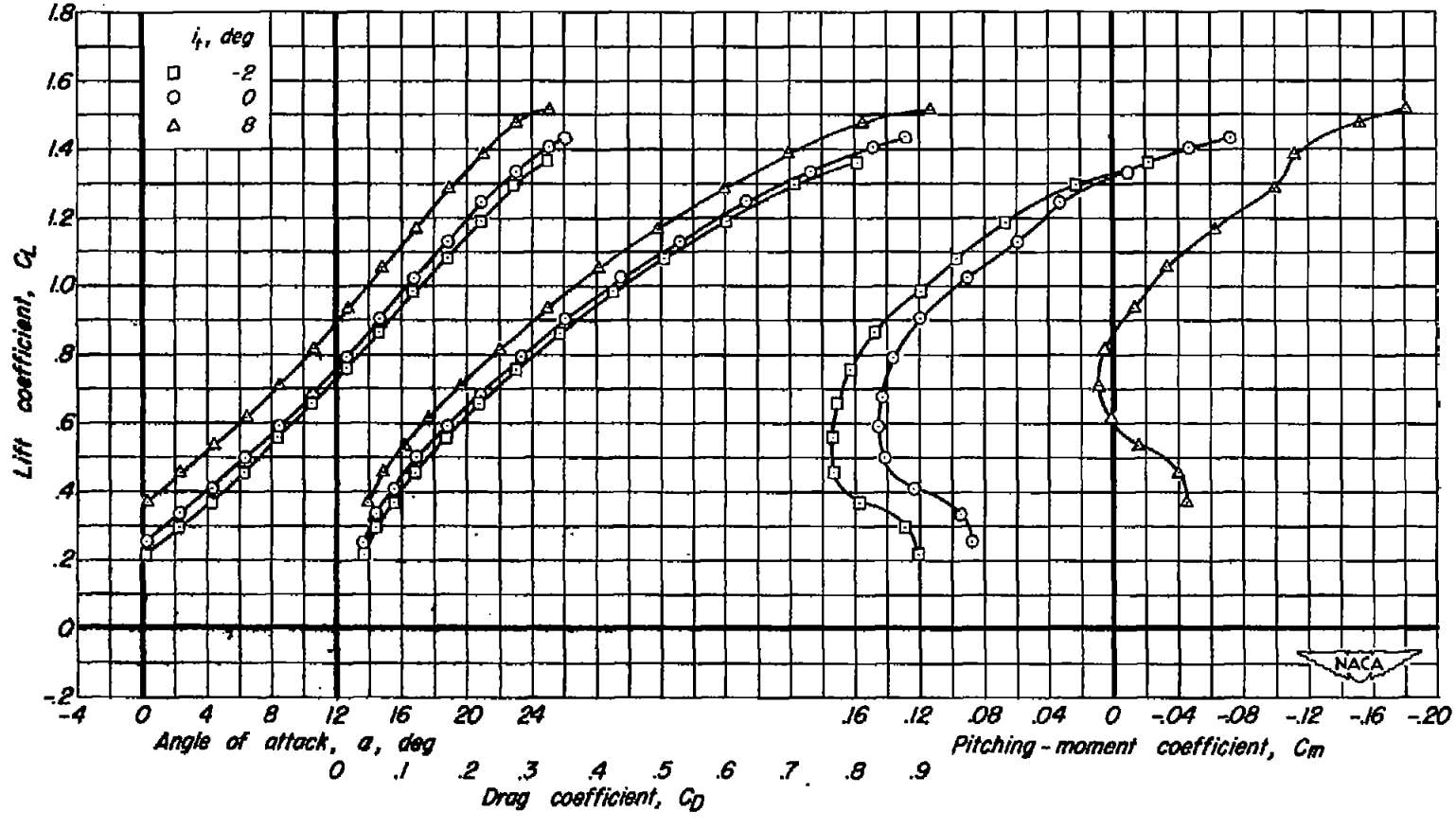

(c) i_w, 10°; δ_f, 0°

Figure 10.- Continued.

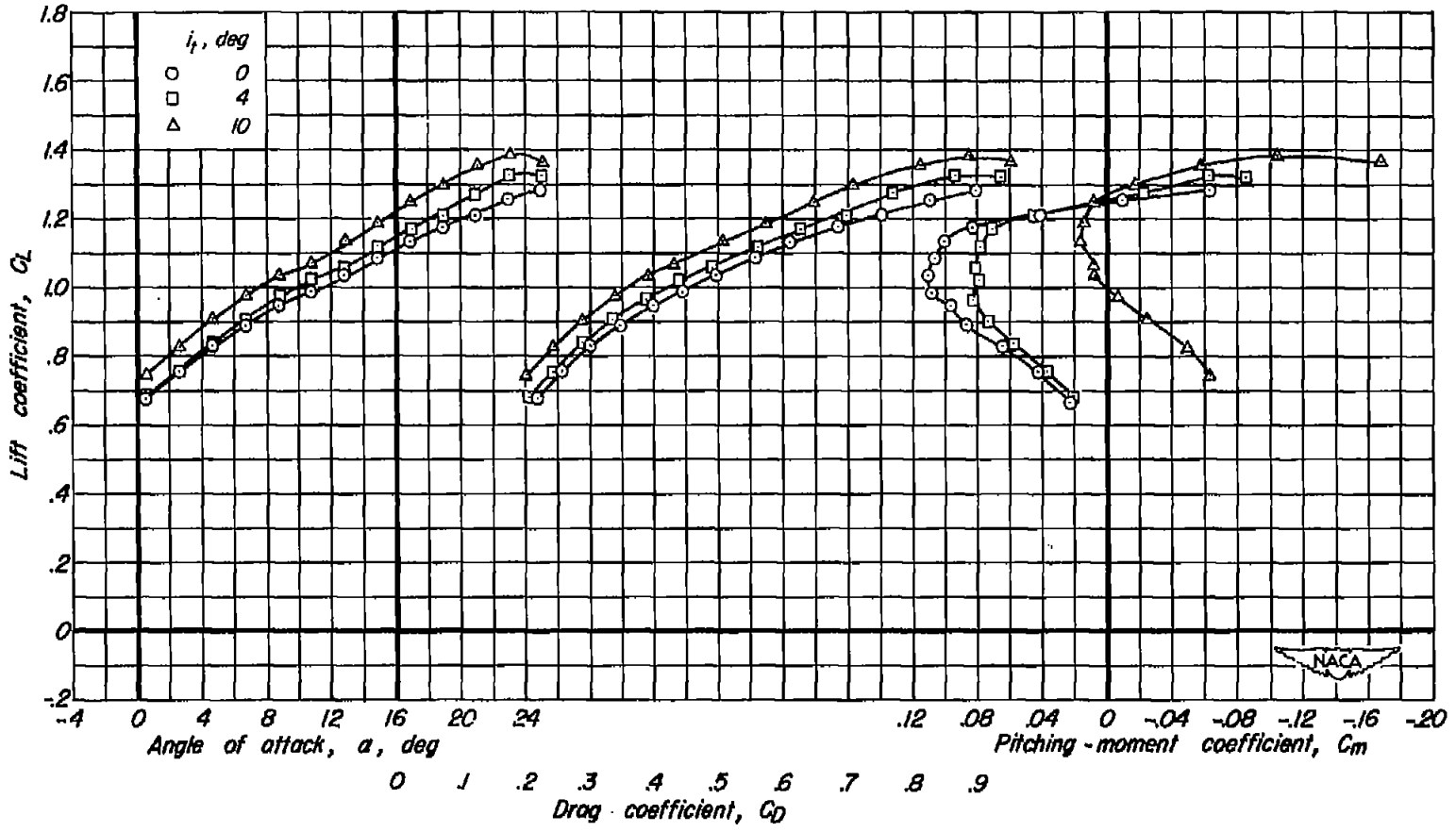

(d) i_w, 10°; δ_f, 40°

Figure 10.- Concluded.

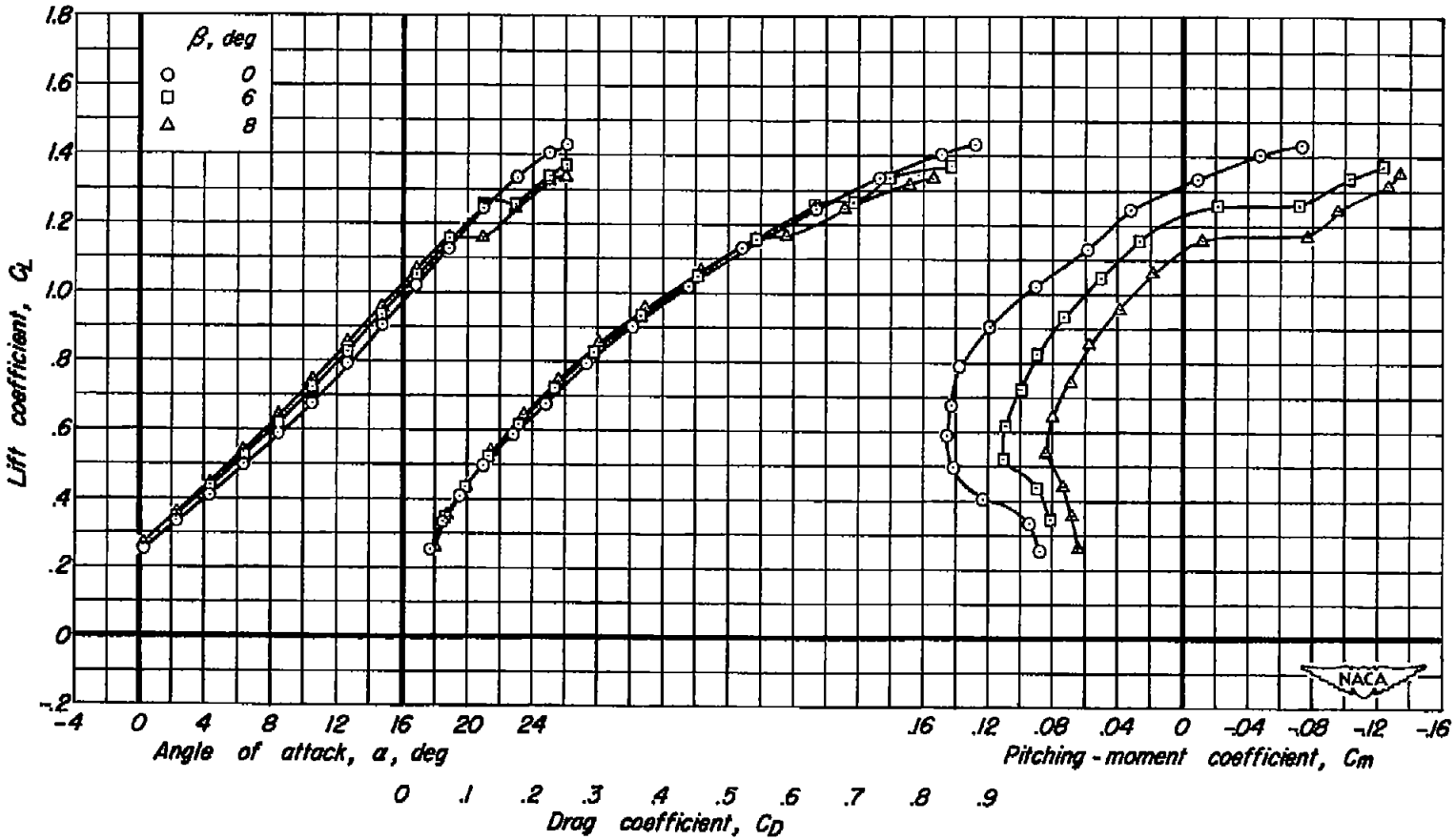

(a) C_L vs α, C_D, C_m

Figure 11.- Characteristics of the complete model at three angles of sideslip with the horizontal tail in the low position; i_w, 10°; δ_f, 0°; i_t, 0°; z/(b/2), 0; moment center, 0.418$\bar{c}$.

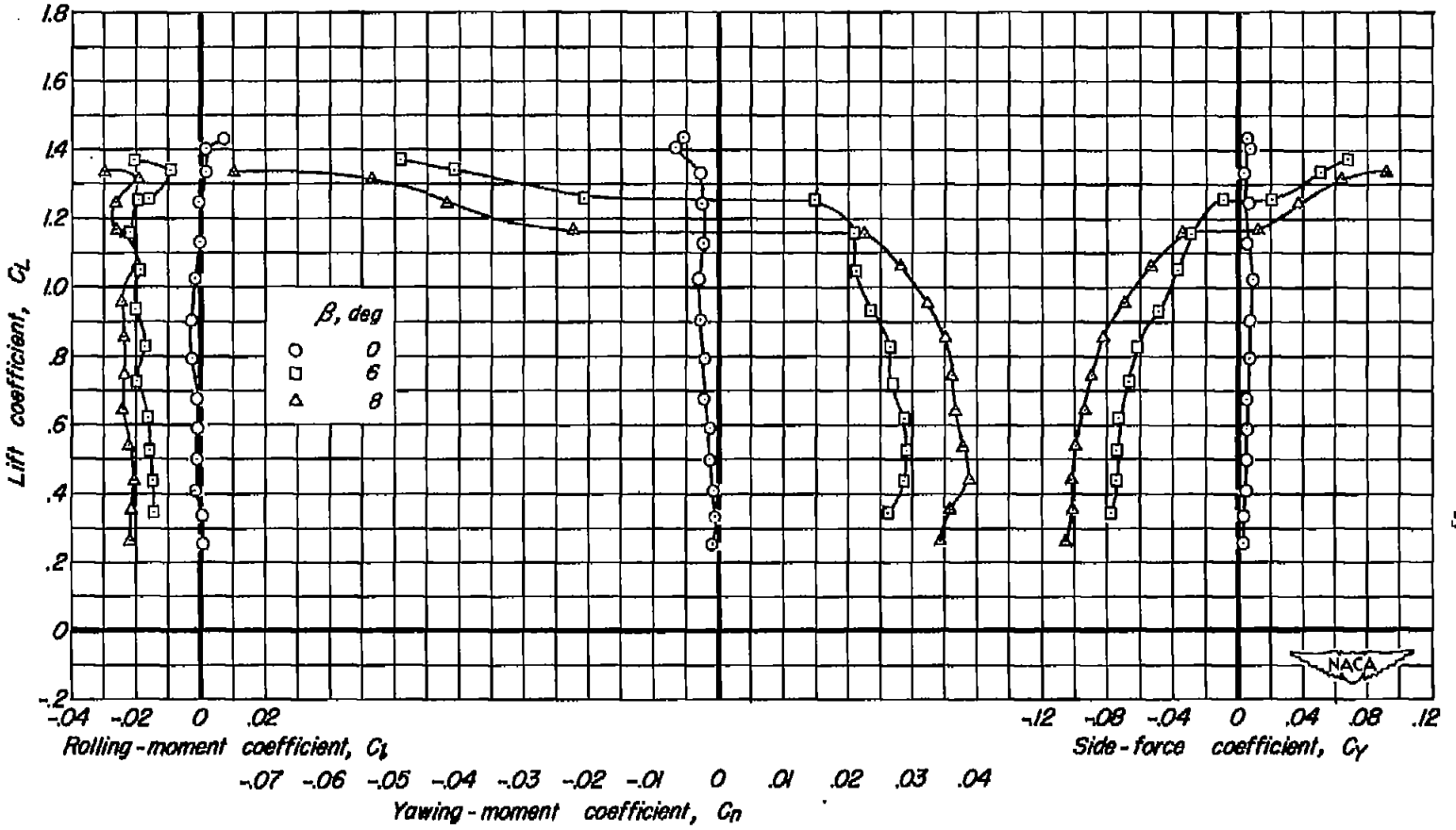

(b) C_L vs C_l, C_n, C_Y

Figure 11.- Concluded.

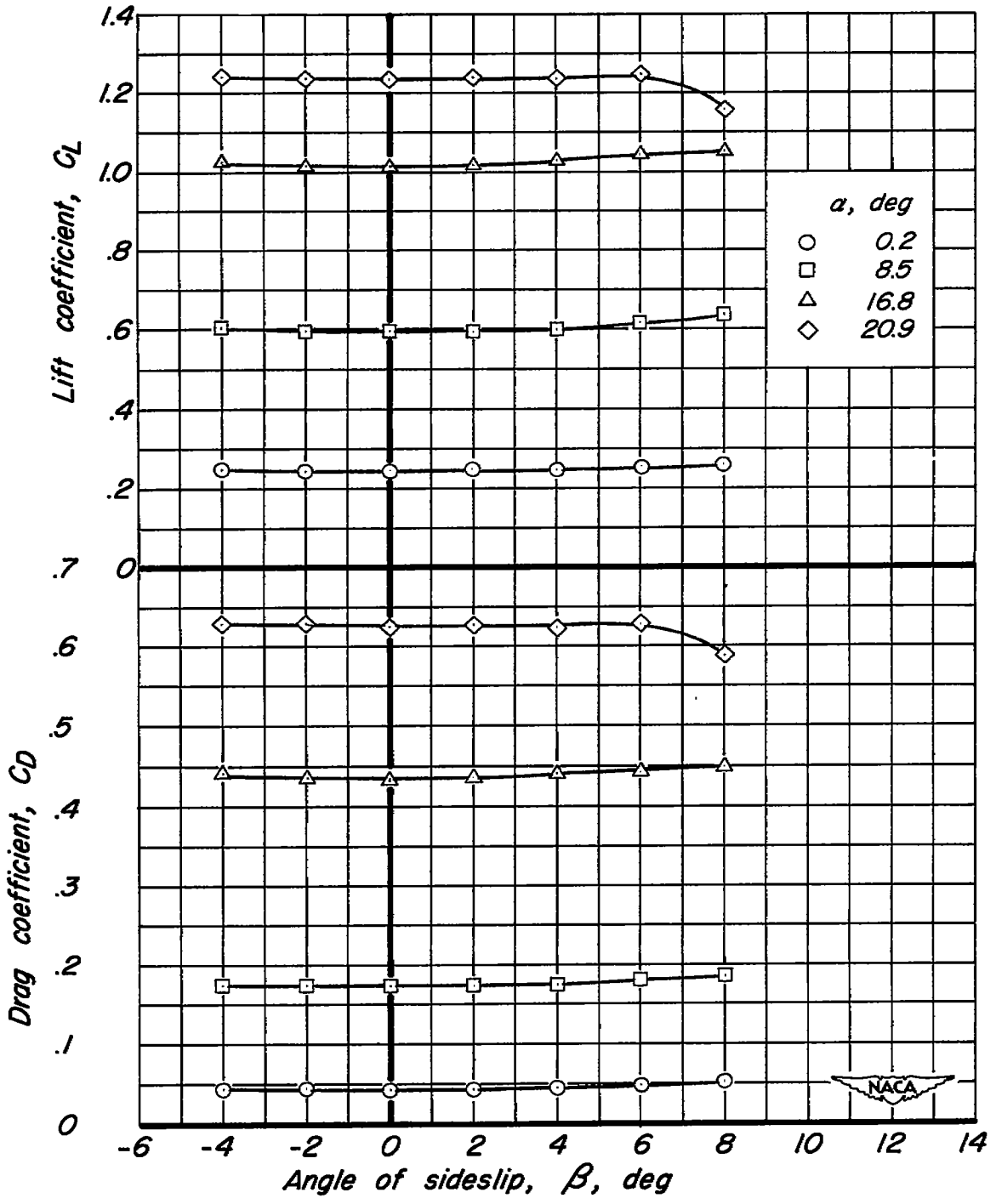

(a) C_L, C_D vs β

Figure 12.- Characteristics of the complete model in sideslip with the horizontal tail in the low position; i_w, 10°; δ_f, 0°; l_t, 0°; z/(b/2), 0; moment center [redacted]

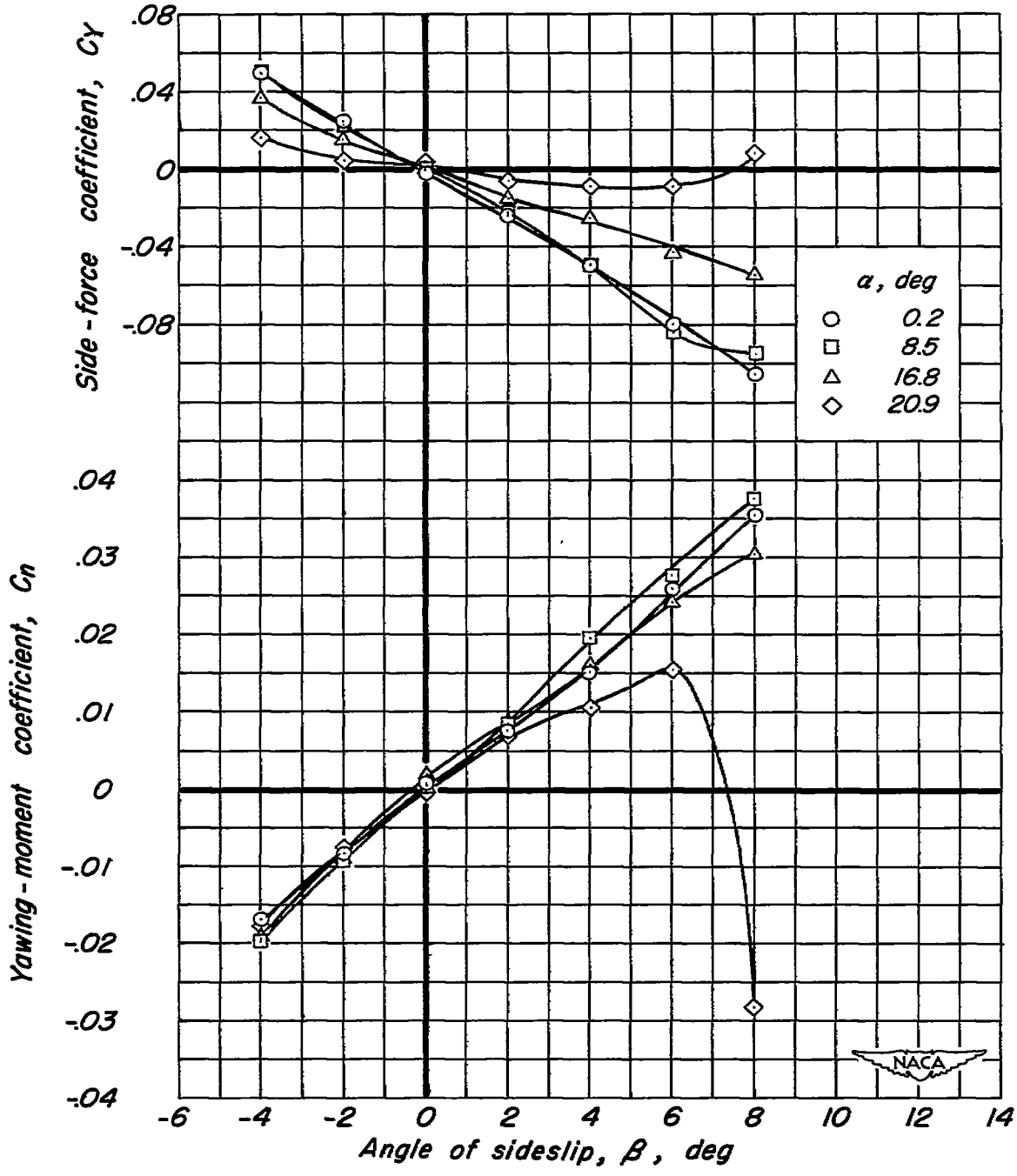

(b) C_y, C_n vs β

Figure 12.- Continued.

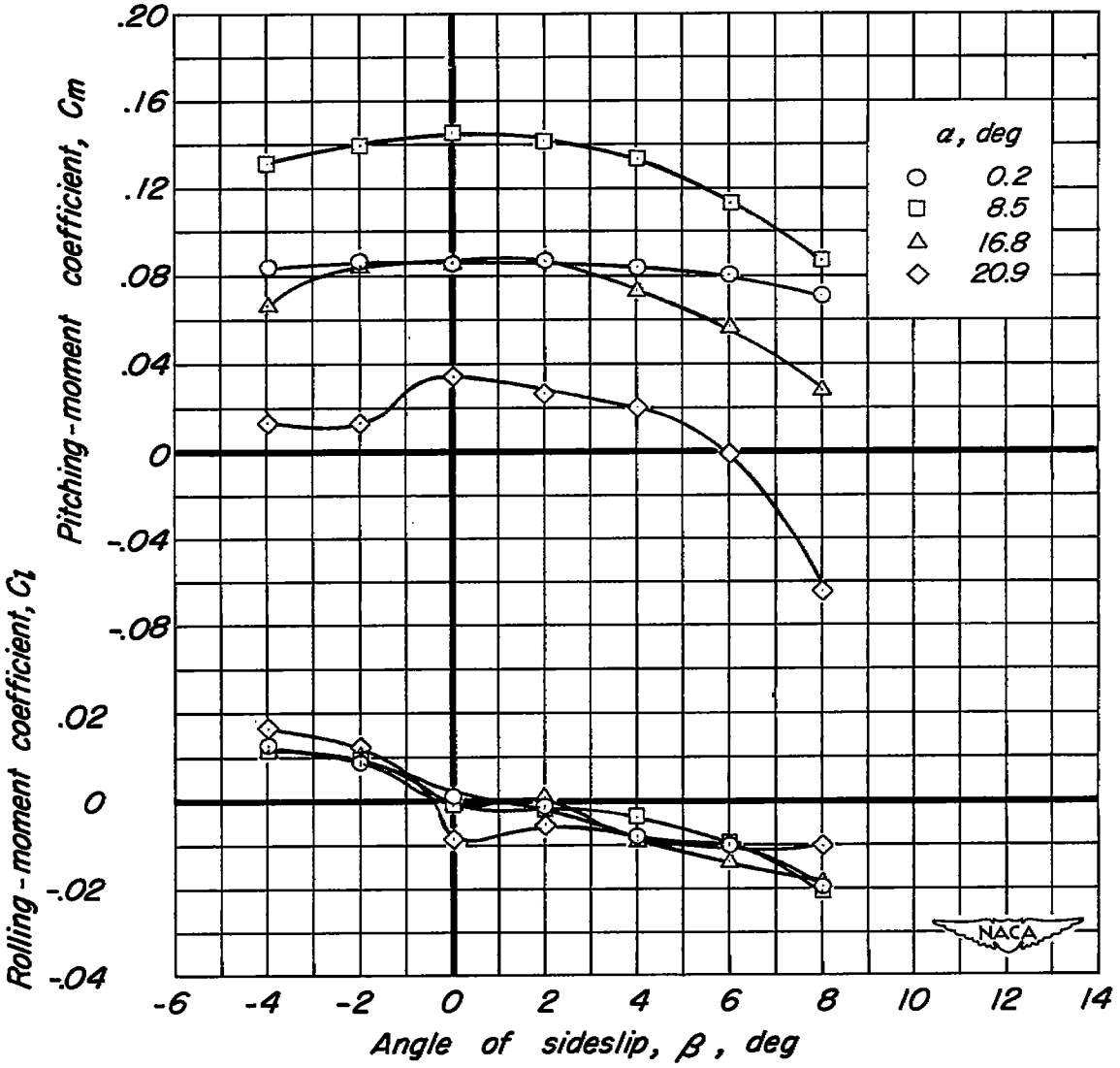

(c) C_m, C_l vs β

Figure 12.- Concluded.

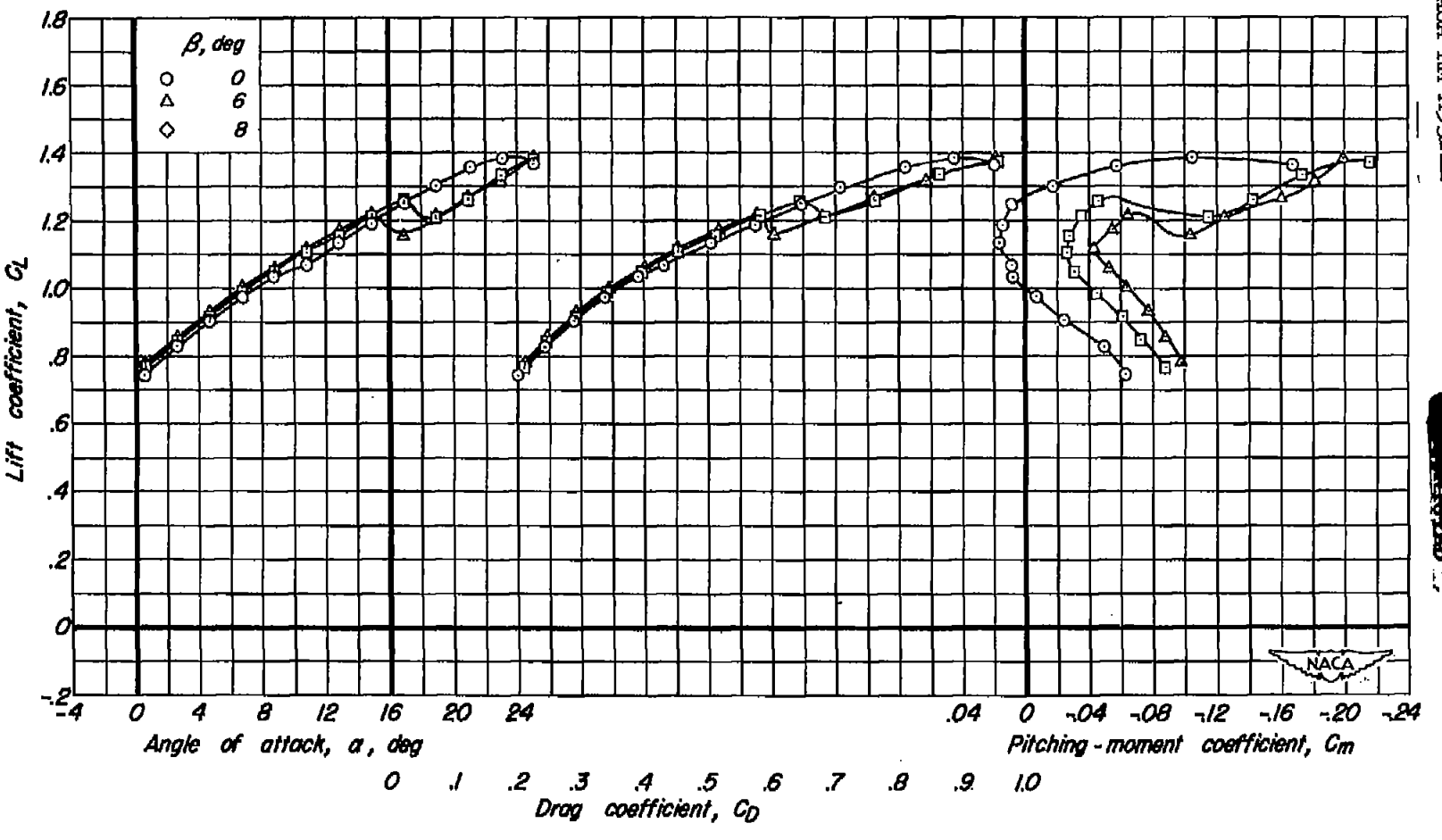

(a) C_L vs α, C_D, C_m

Figure 13.- Characteristics of the complete model at three angles of sideslip with the horizontal tail in the low position; i_w, 10°; δ_f, 40°; i_t, 10°; z/(b/2), 0; moment center, 0.418$\bar{c}$.

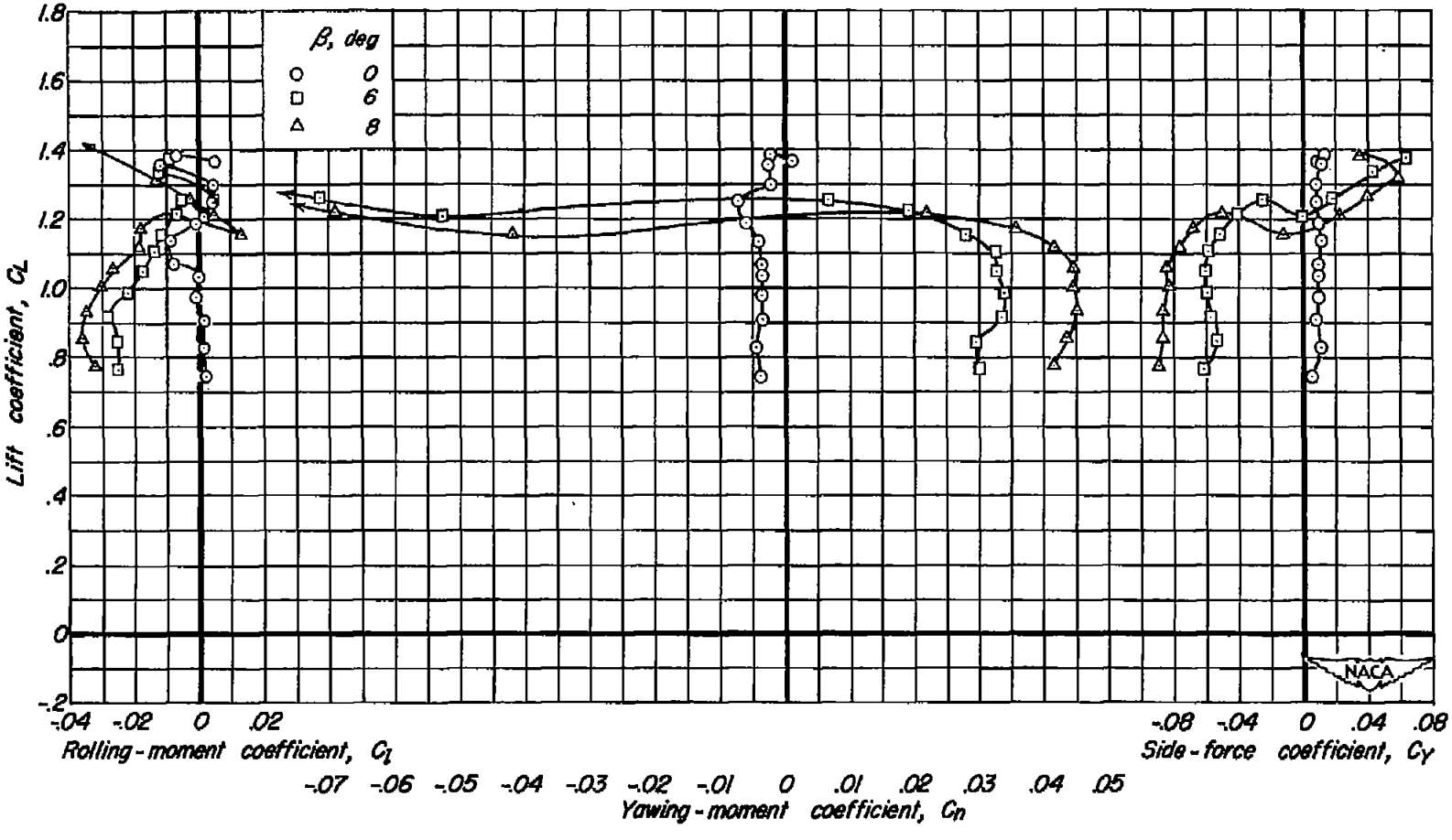

(b) C_L vs C_l, C_n, C_y

Figure 13.- Concluded.

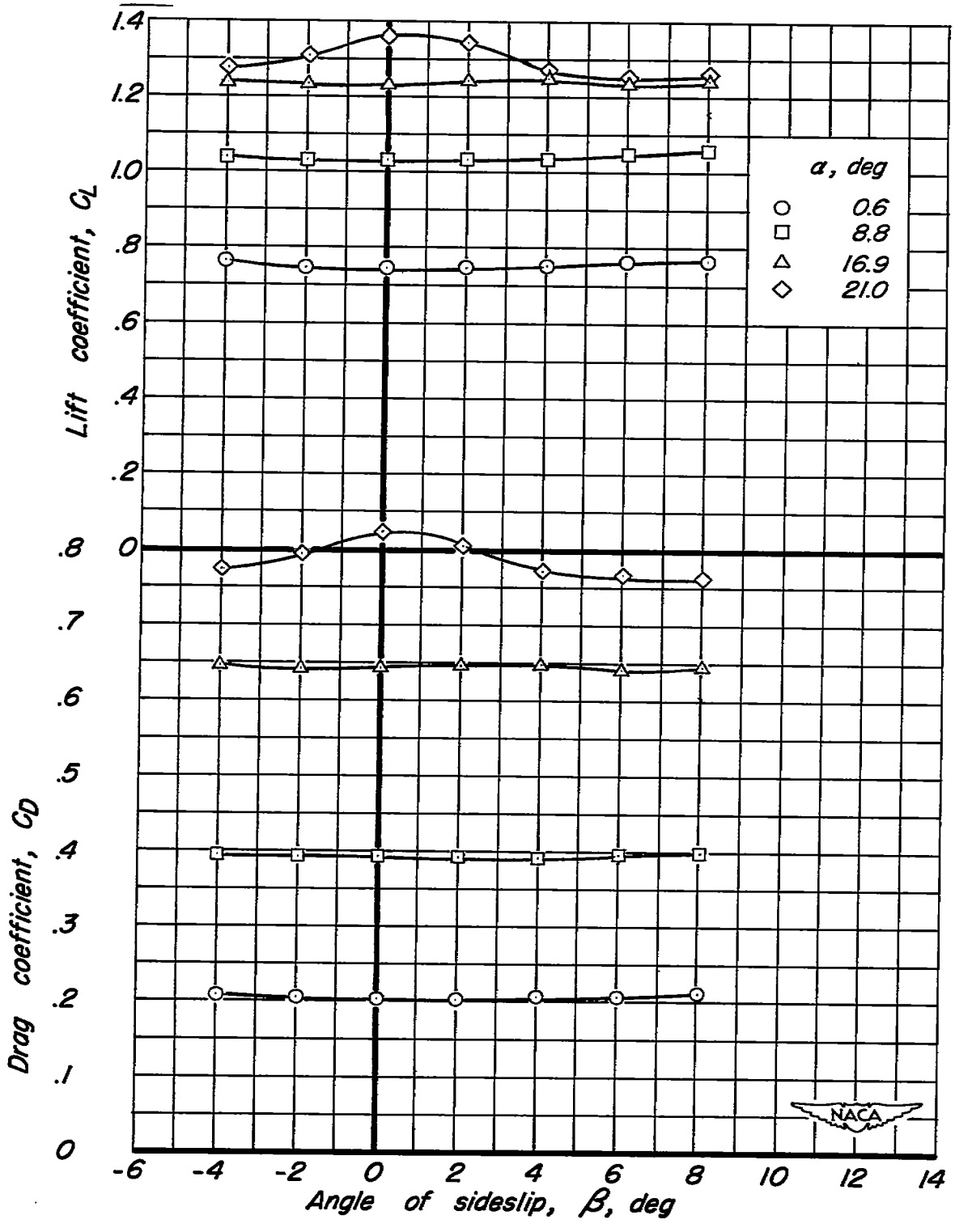

(a) C_L, C_D vs β

Figure 14.- Characteristics of the complete model in sideslip with the horizontal tail in the low position; i_w, 10°; δ_f, 40°; i_t, 10°; z/(b/2), 0; moment center, 0.418$\bar{c}$.

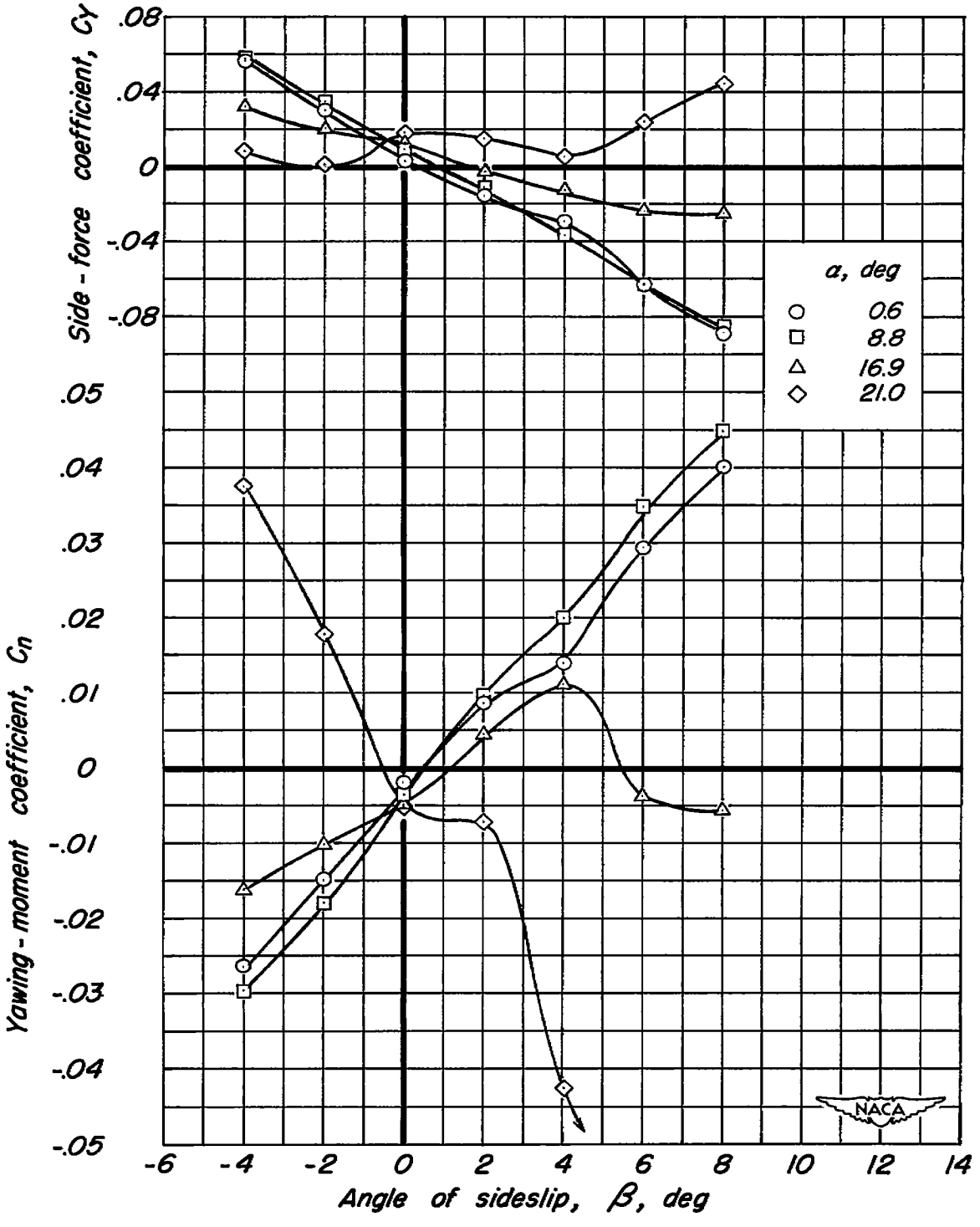

(b) C_y, C_n vs β

Figure 14.- Continued.

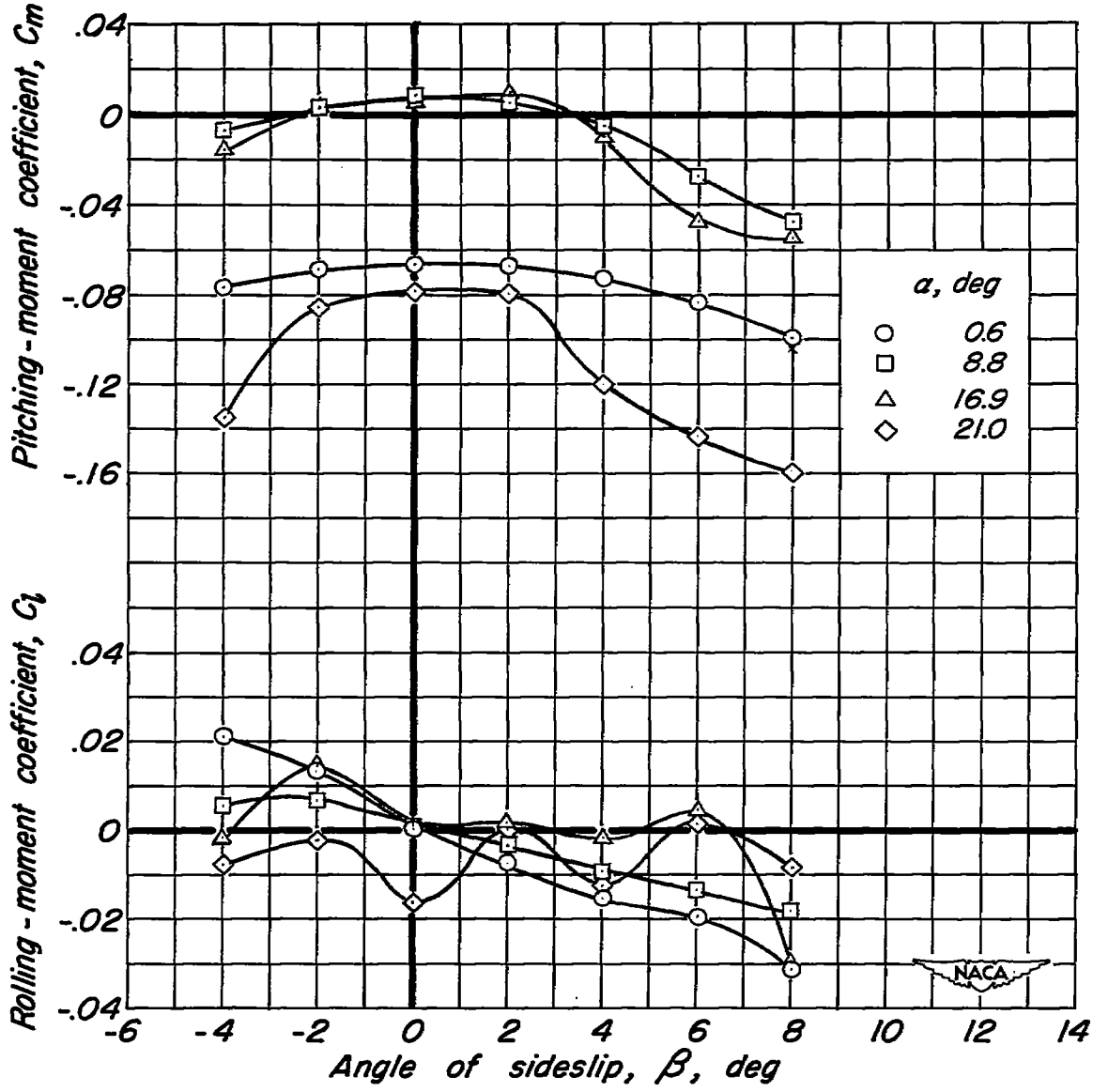

(c) C_m, C_l vs β

Figure 14.- Concluded.

[redacted]

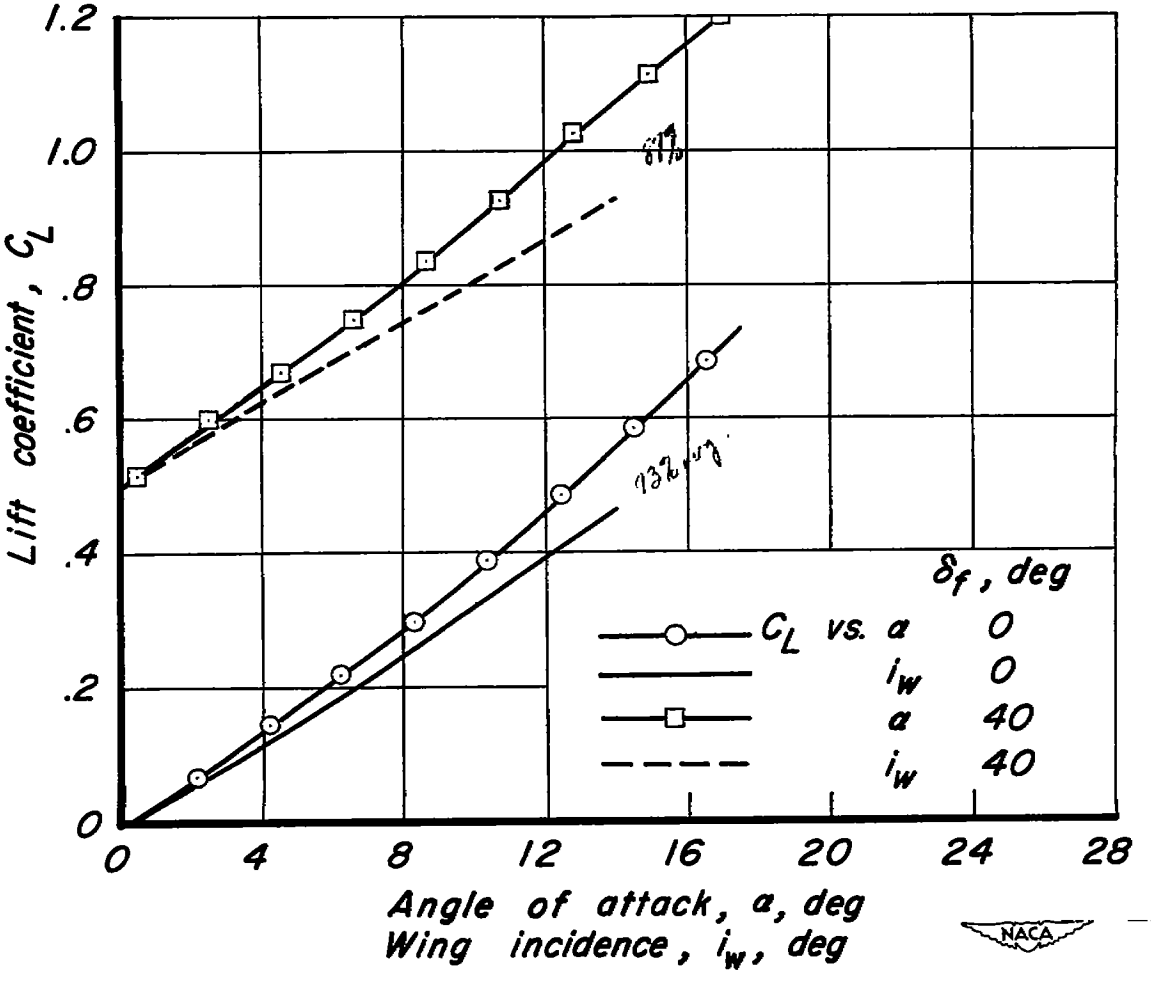

Figure 15.- A comparison of the variations of C_L with α at zero i_w and of C_L with i_w at zero α for the model with the tail off.

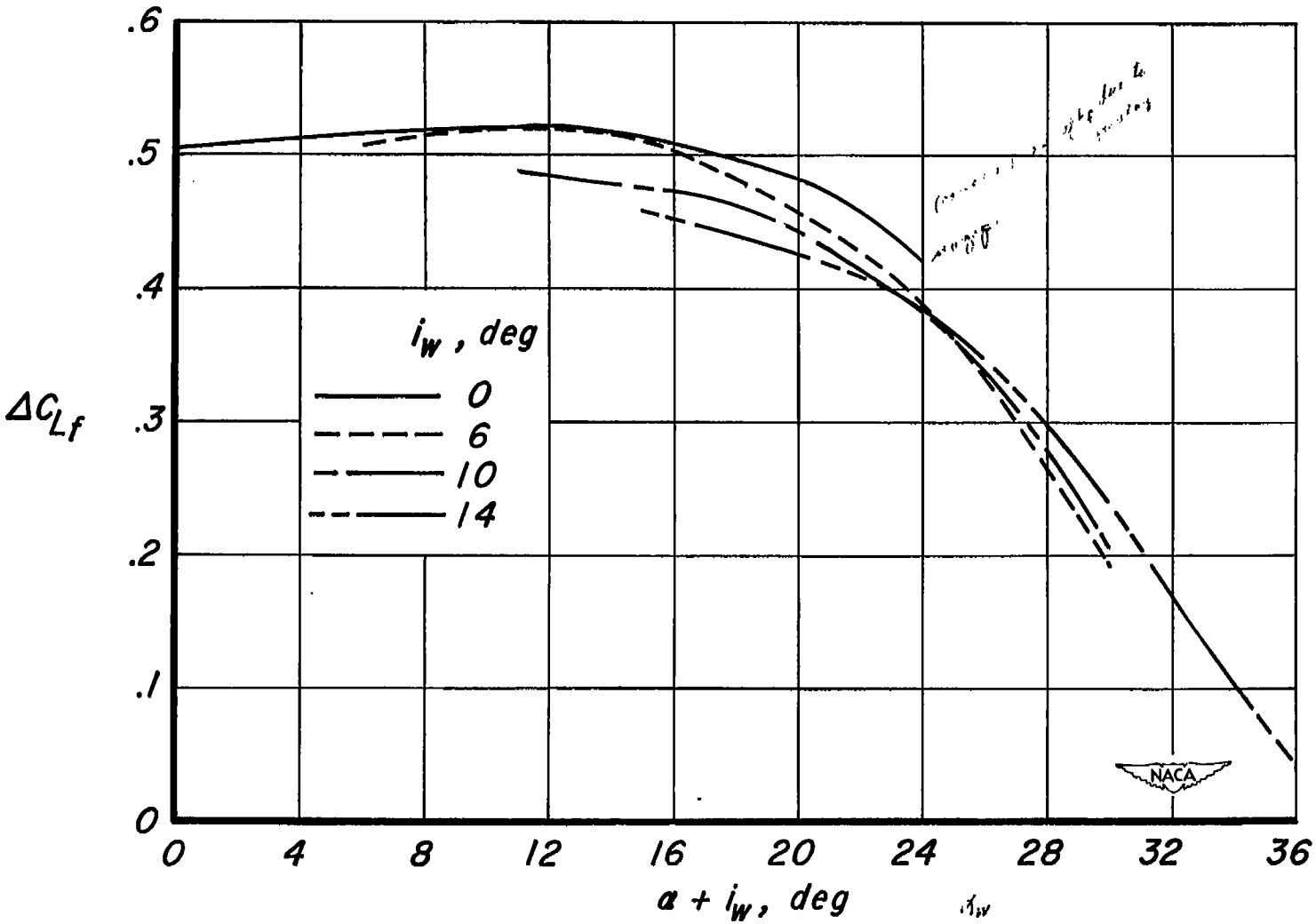

Figure 16.- The effect of wing incidence on the lift increment due to 40° flap deflection for the model with the tail off.

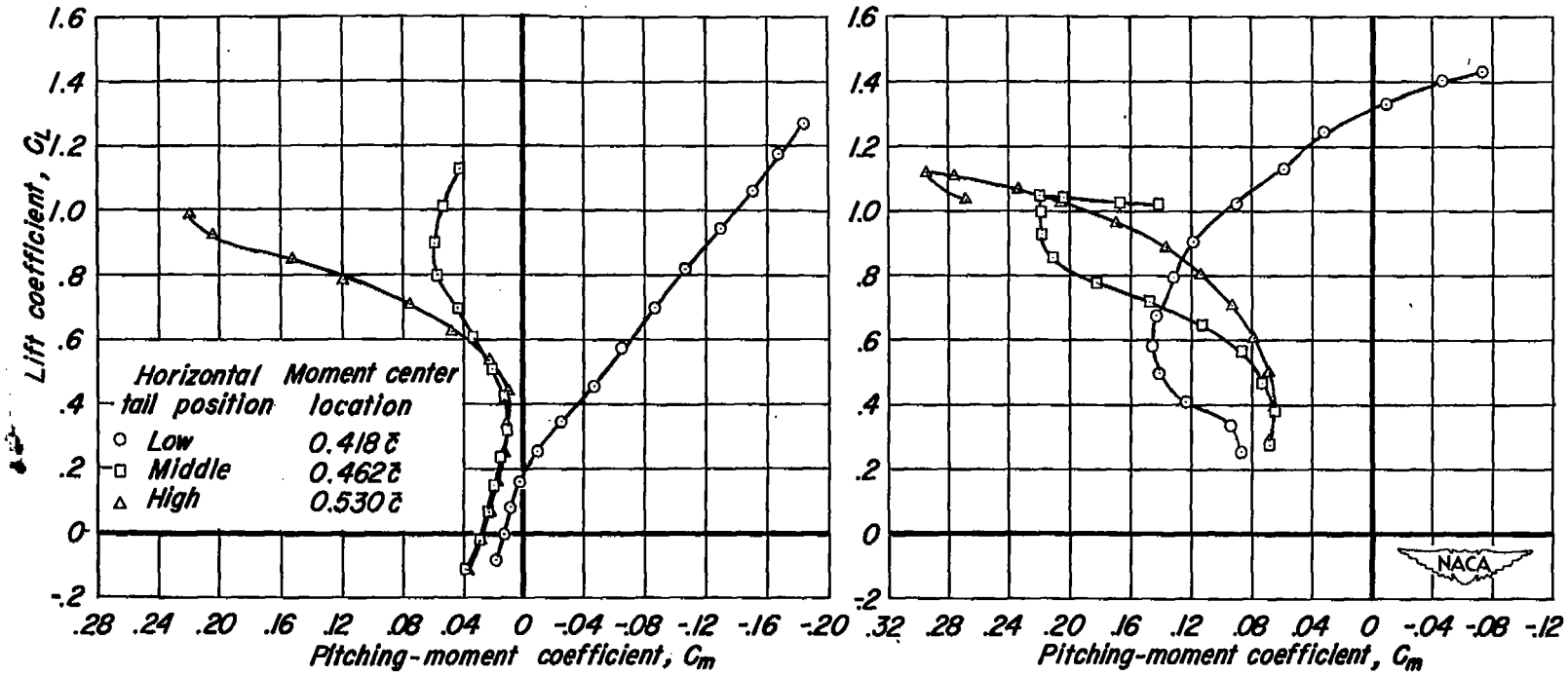

(a) i_w, 0°

(b) i_w, 10°

Figure 17.- The effect of tail position on the pitching-moment curves with flaps undeflected, 0° tail incidence, and two wing incidences.

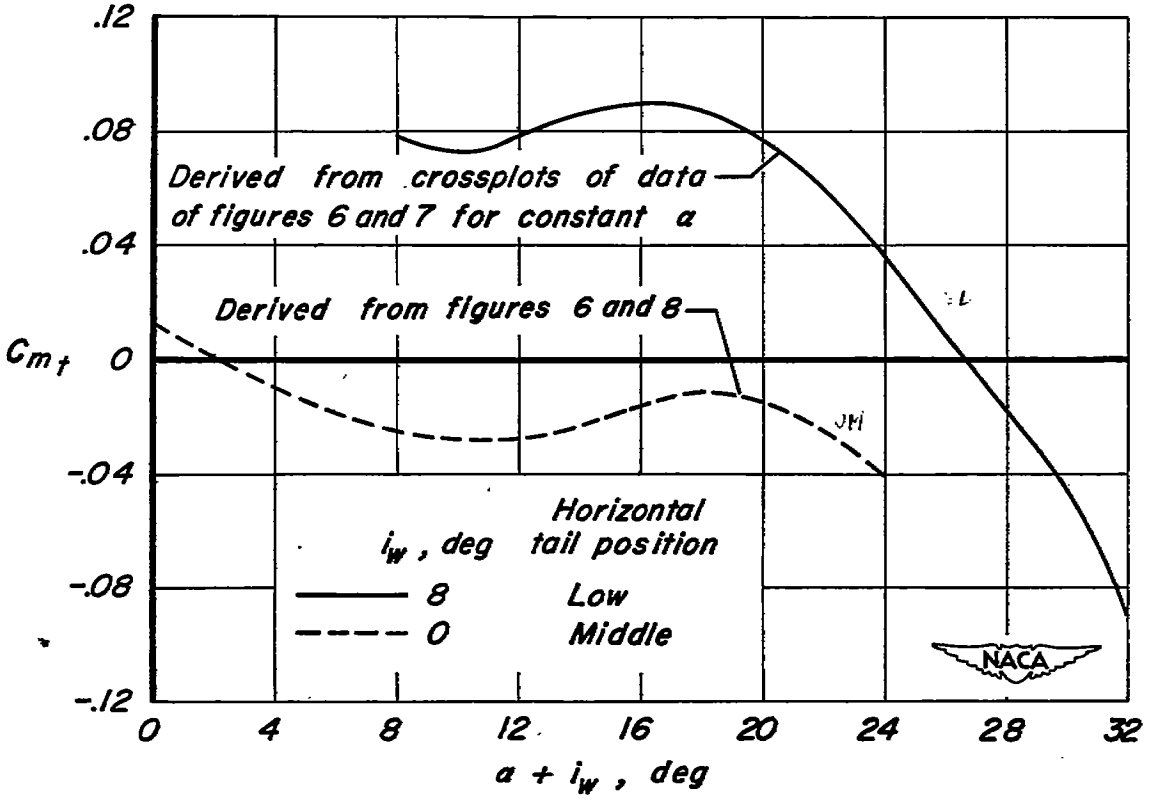

Figure 18.- The pitching-moment contribution of the horizontal tail for a given tail height above the wing-chord plane obtained by wing incidence with the tail fixed as well as by tail position with the wing fixed; moment center, 0.418$\bar{c}$; z/(b/2), 0.25; i_t, 0°.

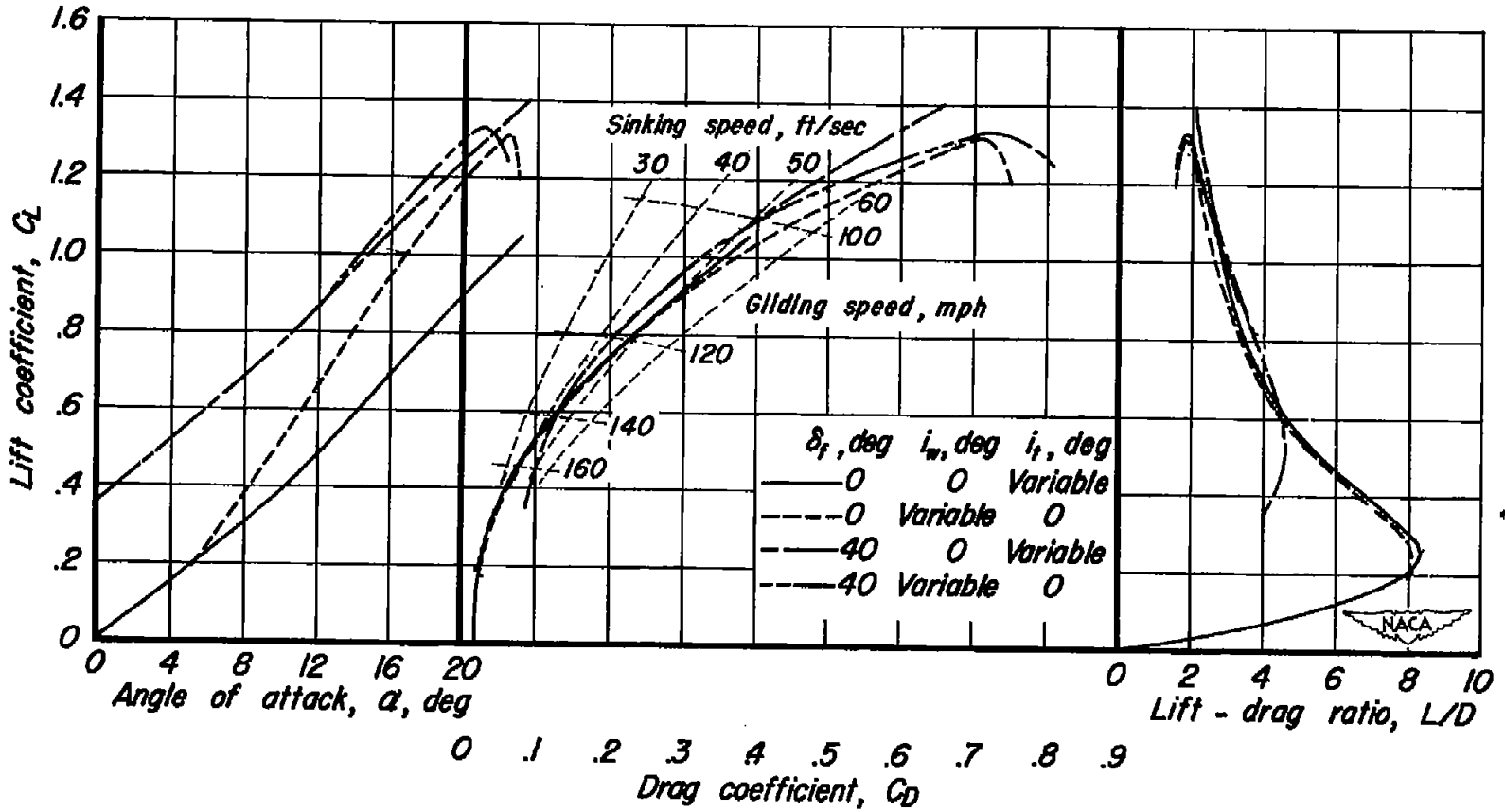

Figure 19.- The longitudinal trim characteristics for the model with the horizontal tail in the low position. Gliding and sinking speed curves were computed using a wing loading of 30 lb/sq ft; moment center, 0.418$\bar{c}$.